MONTE CARLO SIMULATION OF ELECTROMAGNETIC CASCADES IN THE EXTRAGALACTIC INFRARED BACKGROUND

Honours Thesis

DEPARTMENT OF PHYSICS AND MATHEMATICAL PHYSICS
UNIVERSITY OF ADELAIDE

By
Matthew Thomas Whiting
Supervisor: Dr. R.J. Protheroe

November 1996

Abstract

The detection by EGRET of 40 active galactic nuclei in high energy gamma rays ahs sparked interest in high energy extragalactic gamma ray astronomy. However, the presence of the extragalctic infrared background limits the visibility of distant TeV gamma ray sources. In this thesis I investigate the infrared background, the interactions by which it absorbs gamma rays, and I develop a program that uses monte carlo techniques, as well as suitable approximations to model the effect of these interactions on gamma ray spectra, and discuss the implications for high energy gamma ray astronomy.

Acknowledgements

I would like to thank first of all my supervisor, Dr. Ray Protheroe, for his invaluable help and patience all through this year. I also want to thank the various members of the astrophysics group who have given me assistance and support over the year, particularly Troy and Ken. I also must thank the rest of the '96 honours class, for all their support, friendship and general entertainment over the year. Finally, I want to thank my family for putting up with me for the past year.

Contents

Abstract **ii**

Acknowledgements **iii**

1 Introduction **1**

2 High Energy Gamma Rays **3**

3 Infrared Background **6**
3.1 Intensity at $60\mu m$ 6
3.1.1 Background 6
3.1.2 Results 8
3.2 Observational results 10
3.3 Theoretical Predictions 12
3.4 Microwave Background 13

4 Interactions **15**
4.1 Introduction 15
4.2 Cross sections 15
4.2.1 Photon-photon pair production cross sections 15
4.2.2 Inverse compton scattering cross sections 17
4.3 Interaction lengths 17
4.3.1 Interaction lengths for pair production 19
4.3.2 Interaction lengths for inverse compton scattering 20
4.4 Geometry of Interactions 22
4.4.1 Pair production 22
4.4.2 Inverse compton scattering 25

5 Monte Carlo methods **28**
5.1 Introduction 28
5.2 Interaction length 28
5.3 Soft photon energy 29
5.4 Interaction angle 30
5.5 Scattering Angle 31
5.5.1 Pair production 32
5.5.2 Inverse compton scattering 33
5.6 Azimuthal angle 36

6 Electromagnetic cascades **37**
6.1 Program structure . . . 37
6.2 Mono-energetic cascades . . . 39
6.3 Propagation of a power law spectrum . . . 42
6.4 Results . . . 43
6.4.1 Cascading in the microwave background . . . 43
6.4.2 Cascading in the infrared background . . . 44

7 Conclusions **46**

Bibliography **47**

A Cosmological parameters **49**

B Background intensity program **51**

C Cascade program **56**

D Mean free path and mean photon energy program **69**

E Median scattering angle program **74**

Contents

Chapter 1

Introduction

The discipline of high energy gamma ray astronomy has received a major boost in recent years following the success of the Compton Gamma Ray Observatory satellite, which discovered gamma ray emission from over 40 active galactic nuclei (AGN). However, it has long been realised that the gamma ray absorption by the background radiation in infrared and microwave frequencies would limit the visibility of the universe at these gamma ray energies, and this has been demonstrated to some extent by the lack of detection at higher energies of all but one of the AGN detected by the CGRO. In this thesis, I investigate the processes that lead to attenuation of gamma ray emission in both the cosmic microwave background (CMB) and the infrared background (IRB), and develop a method of calculating the expected spectra observed at Earth.

The infrared background is important in determining the visibility of active galaxies at TeV energies – energies that are able to be observed by ground-based telescopes – since gamma rays of these energies will be absorbed to some extent by the IRB. The degree of absorption depends on the distance to the source and the intensity of the IRB. There have been a number of predictions in recent years of the form the IRB spectrum takes, and in Chapter 3 I will look at several of these, compare them with recent observations and investigate how one of them affects gamma ray propagation.

To model the effect of a radiation field on gamma ray emission, one needs to account for at least two processes. The main absorption process is photon- photon pair production, where a gamma ray interacts with a microwave or infrared photon to produce an electron-positron pair. Gamma rays can be created by the process of inverse compton scattering, whereby a high energy electron scatters a low energy photon up to gamma ray energies. These two interactions can combine and feed each other to produce a cascade of electrons, positrons and photons. The theory of these interactions will be discussed in Chapter 4, including how the energies of the final particles are calculated.

These processess have an inherent random nature, and in order to model them using a computer program, one generally needs to sample these random parameters from the relevant distribution. In Chapter 5, I will detail the methods I used to calculate these parameters, using both the correct sampling techniques for the required distributions, as well as using approximations for this sampling in the form of the mean or median value of the distribution.

In Chapter 6, I will show how a complete program may be constructed to model these cascades, using the routines mentioned above. I then show how this program may be used to simulate cascades through either the CMB or the IRB over a given distance, and calculate the resulting spectrum of gamma rays that would be observed on Earth.

The results generated by this program show that pair production in the IRB has important implications for the study of high energy gamma ray emission. In particular, the IRB places an upper limit of about 30 TeV on the energies that will be observed from extragalctic sources, in particular the AGN that were observed by EGRET at GeV energies. This limit applies to the closest EGRET AGN (named Markarian 421), and will decrease for AGN at greater distances. This is in accord with the lack of detection of all EGRET AGN except for Markarian 421 at energies greater than the limiting energy of EGRET.

Chapter 2

High Energy Gamma Rays

The study of high energy (E > 100 MeV) gamma ray emission has risen in importance in the past five years, since the launch of the Compton Gamma Ray Observatory (CGRO) in 1991, along with the development of sensitive atmospheric Cerenkov detectors such as the Whipple observatory in the USA.

Our knowledge of high energy gamma ray sources has been vastly increased by the Energetic Gamma Ray Experiment Telescope (EGRET) on board the CGRO. EGRET is a multi-level spark chamber that detects gamma rays by converting them into an electron-positron pair and following the paths of these particles through the spark chamber. It has a number of levels to determine the direction the gamma ray came from, and this allows it to image strong sources to within 5 arc minutes (1 arc minute = 1/60 degree). This means it is able to pinpoint fairly accurately any gamma ray emission and allow it to be identified with known objects.

EGRET has detected more than 40 active galactic nuclei (AGN) in high energy gamma rays, ranging in energy from 30 MeV to EGRET's limit of 30 GeV (Thompson et al. [1]). The locations of these are shown in Fig. 2.1, along with a small number of Galactic gamma ray pulsars, as well as many sources that are yet to be identified with any other known objects. Also shown is the location of the Large Magellanic Cloud (LMC). Note that most of the unidentified sources are situated in or near the Galactic plane, indicating that they are quite likely in the Galaxy. The sources identified with AGN are located fairly uniformly about the sky, as you would expect for extragalactic sources.

AGN is a broad name for a class of extragalactic sources that are characterised by bright, variable central nuclei. AGN are observed in most regions of the spectrum, notably in radio frequencies, where many AGN are particularly bright radio galaxies. A key feature of many AGN are large jets of relativistic matter that shoot out from either side of the galaxy. These jets originate near the nucleus, which is generally thought to be a supermassive black hole accreting matter from the galaxy. These jets are mostly seen in radio frequencies, where they are very visible due to synchrotron emission from electrons caught up in the magnetic fields carried by the jet.

Most AGN associated with gamma ray emission are a type of AGN termed *blazars*. These are sources characterised by a strongly polarised and often variable optical emission and a flat radio spectrum. This means that the radio spectrum is represented by a power law: $S(\nu) \propto \nu^{-\alpha}$, where α is the spectral index and has a value $\alpha \leq 0.5$ over a given range of frequencies (usually 100 MHz to 30 GHz). In blazars, the jets are aligned very close to the line of sight, and it is thought that the gamma ray emission originates in or near these jets, due to the relativistic beaming of particles caused by the jet motion. A summary of the properties of gamma ray AGN is given by Dermer and Schlickheiser [3].

Figure 2.1: EGRET's observations, showing locations of identified AGN, as well as gamma ray pulsars in the Galaxy, and a number of sources yet to be identified. The map is in Galactic coordinates, with the Galactic centre in the middle of the map, and the plane of the Galaxy extending along the centre horizontal line.

Most of the AGN observed by EGRET have spectra that are well represented by a power law, where the number of photons per unit energy is given by $dN/dE \propto E^{-\alpha}$, where α, the spectral index, is typically between 1.4 and 3.0, with most from 2.0 to 2.4 (von Montigny et al. [2]). Note that for gamma rays, the spectrum is represented by dN/dE, the photon count per unit of energy, since the flux of gamma rays is small enough and the energy of the individual photons is high enough to talk about the actual photon count. In the radio part of the spectrum, however, the energies of the individual photons are far smaller, so it is more meaningful to talk about the emission in terms of electromagnetic waves, leading to the use of the intensity $S(\nu)$ in describing the spectrum.

The spectra of blazars are relatively flat (i.e. not decreasing too rapidly with energy), indicating that emission could extend well into TeV energies and higher (1 TeV = 10^{12} eV). In fact, one of the EGRET sources, the BL Lac object Markarian (Mrk) 421, has been detected at TeV energies by both the Whipple observatory (Punch et al. [4]) and the HEGRA experiment in the Canary Islands (Petry et al. [5]), as has another BL Lac, Mrk 501 (Quinn et al. [6] - Whipple observatory), although this was not detected at GeV energies by EGRET.

The Whipple observatory is located in Arizona, USA. It uses atmospheric Cerenkov imaging to detect gamma rays with energies from 100 GeV to 10 TeV. When a gamma ray enters the atmosphere, it creates a cascade of photons and particles (such as electrons and positrons) by pair production and bremmstrahlung. The particles are generally highly relativistic, and move at a speed greater than the local velocity of light. This causes the emission of Cerenkov light, resulting in a flash of optical light that can be seen by ground-based telescopes. The Whipple observatory is one such telescope, although there are Cerenkov observatories located around the world, including the CANGAROO collaboration at Woomera that the University of Adelaide is involved in.

Mrk 421 remains the only EGRET AGN to have been detected at TeV energies. The reason for this lies in the fact that gamma rays travelling through a radiation field will interact with it and get absorbed. The radiation field relevant for TeV gamma rays is the infrared background (IRB). The average distance gamma rays of these energies travel through the IRB before interacting (known as the mean interaction length) is of the order of 100 Mpc (1 Mpc = 3.26 million light years). This is about the distance to Mrk 421, which is the closest of the EGRET sources. Since the other AGN are much further away, more absorption takes place, making them less likely to be seen at TeV energies.

At higher gamma ray energies (greater than about 0.1 PeV or 10^{14} eV), the cosmic microwave background (CMB) becomes the dominant source of absorption. The number density of photons in the CMB is much greater than that of the IRB, so an interaction is much more likely to occur. This means that the mean interaction length in the CMB is much shorter (by up to several orders of magnitude) than in the IRB. (See Chapter 4 for details on the mean interaction length.)

Thus, at PeV energies, the distances over which absorption becomes important are much shorter. This has the effect of ruling out the possibility of detecting any PeV emission from even the closest AGN (such as Mrk 421). It also means that relatively close objects, such as some of those in our Galaxy or in the Magellanic Clouds, will be affected by absorption due to the CMB. It is unclear, however, what sources, if any, there are of PeV gamma rays in these regions.

Notable among the Galactic sources is Cygnus X-3, an X-ray binary system. It is believed that this system consists of a neutron star (a small, very dense star) orbiting a normal stellar companion. Accretion from the companion onto the neutron star produces the X-rays that were first detected from this system (hence the name: X-3 meaning the third X-ray source found in Cygnus). The neutron star is sufficiently close to the companion that high energy particles emitted by the neutron star may interact with the companion's outer atmosphere, and produce gamma ray emission. This system is far enough away ($\sim$ 10 kpc) for absorption to have a noticeable effect. There have been detections reported of Cygnus X-3 at TeV and greater energies (e.g. Lloyd-Evans et al. [8] and Samorsky and Stamm [9]), although recent observations at TeV and PeV energies (Aglietta et al. [10]) have cast some doubt on the significance of these detections.

Objects of interest in the Magellanic Clouds (at a distance of about 50 kpc) include the X-ray binary systems LMC X-4 and SMC X-1 (which are of a similar type to Cygnus X-3 - a small, dense object orbiting a normal stellar companion), as well as the X-ray pulsar PSR 0540-693 (a neutron star, spinning rapidly and giving off pulsed X-ray emission). Searches have been made attempting to detect TeV or greater energy emission from these objects (Allen et al. [11]), but no significant emission was found.

Chapter 3

Infrared Background

3.1 Intensity at 60μm

3.1.1 Background

It is possible to calculate the background intensity of the infrared background (IRB) at a particular frequency or wavelength fairly easily. In this section I'll briefly describe the background to the calculation of the intensity at a wavelength of 60μm.

There are three quantities used to descibe the amount of radiation from a source - luminosity, flux, and intensity. The luminosity is the rate of energy output from a source. The total luminosity of a source, L is in SI units of W. One can also define the specific, or spectral luminosity L_ν by $L = \int L_\nu d\nu$, with SI units of W Hz^{-1}.

The flux is the energy flow through an area. Here I use the definitions from Rybicki and Lightman [28], where flux is the energy carried by all rays through a given area per unit time. As for luminosity, one can define the total flux, S (sometimes F is used instead), with SI units W m^{-2}, and the specific flux S_ν, defined by $S = \int S_\nu d\nu$, with SI units W m^{-2} Hz^{-1}.

Similar to flux is the intensity, I. This is defined as the energy carried through a given area by rays within an infinitesimal solid angle $d\Omega$. The SI units for I are W m^{-2} sr^{-1}, and the SI units for I_ν (which is defined similarly to L_ν and S_ν) are W m^{-2} Hz^{-1} sr^{-1}. Another unit often used for intensity is the Jansky, Jy, defined as 1 Jy $= 10^{26}$ W m^{-2} Hz^{-1} sr^{-1}. Thus, the units of flux are Jy sr. Throughout this thesis, I_ν, S_ν and L_ν will be refered to as intensity, flux and luminosity respectively, that is, the term "specific" will be dropped.

The key ingredient in calculating the intensity is the luminosity function, $\rho(L_\nu, z)$. This gives the number of sources of luminosity L_ν at a redshift z, per comoving volume, per unit of luminosity. Its units are Mpc^{-3} (W Hz^{-1})$^{-1}$. Comoving volume is a volume in comoving coordinates, defined such that the volume in these coordinates remains constant as the universe expands (i.e. the coordinates move with the expansion). This is different to the normal physical volume, which increases with the expansion. A definition of the comoving volume is given in Appendix A.

A general form of a luminosity function covering sources at all redshifts has three components: the local luminosity function $\rho_0(z)$, dealing with sources at redshift $z = 0$; and functions that deal with the evolution with redshift (i.e. evolution over time). This evolution can described in two different ways. Firstly, the density of the sources can change with time. Since the density is defined as number per comoving volume, the only way for the density to change is for the number of sources to change. This will happen predominantly by the creation of sources (i.e. galaxy formation) and by the merging of galaxies. This form of evolution is described by the function $g(z)$, defined by:

$$\rho(L,z) = g(z) \times \rho(L, z=0)$$

The second form of evolution is how the actual luminosity of the sources changes with time. This is due, for instance, to changes in the physical processes involved in the source. This is described by the function $f(z)$, defined by:

$$L(z) = f(z) \times L(z=0)$$

So, we can combine these two relations, to give an expression for the luminosity function in terms of the local luminosity function at a luminosity L_ν, at frequency ν, and the two evolution functions:

$$\rho(L_\nu, z) = \frac{g(z)}{f(z)}\rho_0\left(\frac{L_\nu}{f(z)}\right) \tag{3.1}$$

As the universe expands, any radiation that has been emitted will be redshifted, meaning its frequency will decrease. Thus, a photon emitted at redshift z, and observed with frequency ν will have been emitted at a frequency $\nu' = \nu(1+z)$. Also, if you observe a flux S_ν, then the luminosity of the source at ν' will be given by

$$L_{\nu'}d\nu' = 4\pi d_{\rm L}^2 S_\nu d\nu$$

$$L_{\nu'} = S_\nu \frac{4\pi d_{\rm L}^2}{(1+z)} \tag{3.2}$$

where $d_{\rm L}$ is the luminosity distance (see Appendix A for full expression of $d_{\rm L}$).

However, since we will want to use L_ν, we need to make use of the spectrum of luminosities, to relate L_ν to $L_{\nu'}$. This is done by assuming a simple power law $L \propto \nu^{-\alpha}$, giving

$$L_\nu = L_{\nu'}\left(\frac{\nu'}{\nu}\right)^\alpha$$

or, using the relation between ν' and ν,

$$L_\nu = L_{\nu'}(1+z)^\alpha \tag{3.3}$$

where α is called the spectral index.

Using the luminosity function, we are able to evaluate the differential source counts. The number of sources with observed flux greater than S_ν at frequency ν is denoted $N(>S_\nu)$. This is given by the integral

$$N(>S_\nu) = \int dz \frac{dV_c}{dz}\int_{L_{\nu'}}^{\infty} dL_{\nu'}\,\rho(L_{\nu'}, z) \tag{3.4}$$

where dV_c/dz is the rate of change of comoving volume with redshift. The differential source count, $n(S_\nu)$ is defined as the number of sources with observed flux in the region $S_\nu \to S_\nu + dS_\nu$ per unit flux, per unit solid angle, with units of Jy^{-1} sr^{-2}. This is related to the derivative of $N(>S_\nu)$ with respect to flux:

$$n(S_\nu) = \frac{1}{4\pi}\frac{dN}{dS_\nu} = \int dz \frac{dV_c}{dz}\frac{d_L^2}{(1+z)}\rho(L_\nu, z)(1+z)^\alpha \tag{3.5}$$

$$\text{where } L_\nu = L_{\nu'}(1+z)^\alpha$$

The extra factor of $(1+z)^\alpha$ comes from the definition of ρ, as being the number of sources per comoving volume, per unit of luminosity. Since $L_\nu = L_{\nu'}(1+z)^\alpha$, we must have

$$\frac{d}{dL_{\nu'}} = (1+z)^\alpha \frac{d}{dL_\nu}.$$

To get the intensity, I_ν (in units of Jy), you simply integrate the sourcecounts over observed flux, to give

$$I_\nu = \int n(S_\nu)\ S_\nu\ dS_\nu \tag{3.6}$$

3.1.2 Results

The calculations that I made were to calculate the intensity at 60μm for different luminosity functions and evolutionary models.

The first luminosity function that I used was the 60μm local luminosity function from Hacking et al. [16]:

$$\rho_0(L_{60}) = 2.94 \times 10^{28} 10^Q \tag{3.7}$$

$$Q = Y - \left[B^2 + \left(\frac{\log L_{60} - X}{W}\right)^2\right]^{1/2} - 2.5 \log L_{60}$$

Here I use the values quoted in Protheroe and Biermann [17], of $B = 1.51$, $W = 0.85$, $X = 23.96$, and $Y = 5.93$. Note that these values assume that $H_0 = 100$ km s^{-1} Mpc^{-1}, and $q_0 = 0.5$. This is the best fit to the data of Soifer et al. [18], as computed by [16]. The data in question are from the Infrared Astronomical Satellite (IRAS) all-sky survey.

There were three types of evolution that I considered with this model, using those considered in [17]. The first is no evolution. This means you set $f(z) = 1$ and $g(z) = 1$, so that:

$$\rho(L_\nu, z) = \rho_0(L_\nu)$$

Secondly, I considered pure luminosity evolution, where $g(z) = 1$ and

$$f(z) = \begin{cases} (1+z_0)^4 & z \geq z_0 \\ (1+z)^4 & z < z_0 \end{cases} \tag{3.8}$$

where I used $z_0 = 0.8$, the best fit given by [17]. Finally, I used the evolution given by Table 1. in Condon [19], which gives values of $\log(f)$ and $\log(g)$ for values of $\log(1+z)$ between 0 and 1.For values of z not listed, the $\log(f)$ and $\log(g)$ values are obtained by interpolating or extrapolating as necessary. These functions are shown in Fig 3.1.

The other luminosity function that I used was the 60μm luminosity function from Saunders et al. [20], with density evolution, given by:

$$\rho(L, z) = (1+z)^{6.7} \rho(L) \tag{3.9}$$

where

$$\rho(L) = \frac{C}{L \log 10}\left(\frac{L}{L_*}\right)^{1-\alpha} \exp\left[-\frac{1}{2\sigma^2} \log_{10}^2\left(1 + \frac{L}{L_*}\right)\right]$$

with: $C = (2.6 \pm 0.8) \times 10^{-2}\ h^{-3}$ Mpc^{-3}, $\alpha = 1.09 \pm 0.120$, $\sigma = 0.724 \pm 0.031$, and $L_* = 10^{(8.47 \pm 0.23)}\ h^{-2}\ L_\odot$. Also note that this requires $H_0 = 66$ km s^{-1} Mpc^{-1}, instead

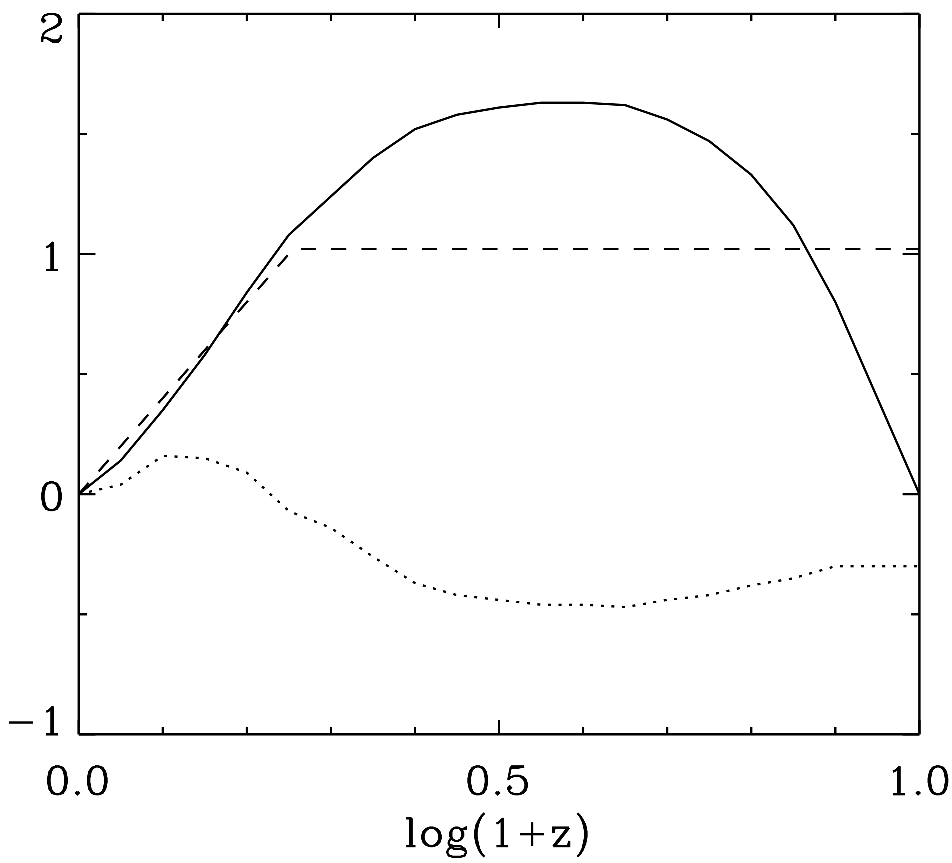

Figure 3.1: Evolution functions. Solid and dotted lines are $\log(f(z))$ and $\log(g(z))$ respectively from Condon [19]. Dashed line is $\log(f(z))$ for the pure luminosity evolution (Eq. (3.8)) of Protheroe and Biermann [17].

of the value of 100 that I was using for the first luminosity function. This will alter the calculations of d_L and dV_c/dz.

The extra $(L\log 10)^{-1}$ factor compared to [20] is because their luminosity function is defined as the differential luminosity function per decade of luminosity, i.e.

$$\begin{aligned} d(\log_{10} L) &= d\left(\frac{\log L}{\log 10}\right) \\ &= \frac{dL}{L\log 10} \end{aligned}$$

so

$$\frac{dN}{d(\log_{10} L)} = \frac{1}{L\log 10}\frac{dN}{dL}.$$

Given a luminosity function and the relevant evolution functions, it is fairly straightforward to calculate the 60μm intensity, using Equations (3.2), (3.5), and (3.6). Care has to be taken, however, when considering the spectral index α (Eq.(3.3)). A source generally does not have a single spectral index, but instead some distribution of indices about some mean. To consider this, I used the following gaussian distribution approximation from Hacking, Condon and Houck [16].

The fraction of sources with given luminosity L and redshift z having spectral index α is well approximated by

$$u(\alpha|L,z) = \frac{1}{\sqrt{2\pi}\sigma(L,z)} \exp\left(\frac{-[\alpha - \langle\alpha(L,z)\rangle]^2}{2\sigma^2(L,z)}\right) \tag{3.10}$$

where $\sigma(L,z) = 0.5$ is the dispersion and $\langle\alpha(L,z)\rangle$ is the mean spectral index for a given luminosity and redshift, parametrised by

$$\langle\alpha(L,z)\rangle = \begin{cases} \alpha_{25\mu\mathrm{m}} & \text{for } z > 0.41 \\ \alpha_{25\mu\mathrm{m}} \left[\frac{\log(1+z)}{\log(1.41)}\right] + \alpha_{60\mu\mathrm{m}}(L, z=0) \left\{\frac{\log[1.41/(1+z)]}{\log(1.41)}\right\} & \text{for } z \le 0.41 \end{cases}$$

where

$$\alpha_{60\mu\mathrm{m}}(L, z=0) = \begin{cases} +2.7 & \text{for } L < 10^{22} \\ +2.7 - 0.5\log\left(\frac{L}{10^{22}\ \mathrm{W\ Hz^{-1}}}\right) & \text{for } 10^{22} < L < 10^{25.4} \\ +1.0 & \text{for } L > 10^{25.4} \end{cases}$$

and $\alpha_{25\mu\mathrm{m}} = +2.4$. Here, L is measured in units of W Hz^{-1}

The function $u(\alpha|L,z)$ is effectively a weighting function. We can replace the parts of Eq.(3.5) that depend on α by their weighted mean. Since $L_\nu = L_{\nu'}(1+z)^\alpha$, $\rho(L_\nu, z)$ depends on α, so we replace $\rho(L_\nu, z)(1+z)^\alpha$ by

$$\sum_\alpha \rho(L_{\nu'}, z)(1+z)^\alpha\ u(\alpha|L_{\nu'}, z).$$

Note that $L_{\nu'}$ is the luminosity at *emission*.

From here it is fairly straightforward to calculate the differential sourecounts $n(S_\nu)$ as a function of S_ν, using Eq. (3.5), for the different evolutionary models discussed earlier. These are shown in Fig. 3.2.

Similarly, the intensity can be calculated by integrating the sourcecounts according to Eq.(3.6). I integrated this over the range of S_ν values shown in Fig. 3.2, i.e. $S_\nu = 10^{-2}$ to $S_\nu = 10^2$ (in the case of the luminosity function from Saunders et al. [20], the minimum value of S_ν is 0.6). This gives the following results for the intensity at 60μm (5×10^{12} Hz):

Model	I_ν (W m^{-2} Hz^{-1} sr^{-1})
No evolution	1.55×10^{-21}
Pure luminosity evolution (Eq. (3.8))	3.69×10^{-21}
Evolution from Condon [19]	4.27×10^{-21}
Luminosity function from Saunders et al. [20]	1.51×10^{-22}

The program used to calculate the pure luminosity evolution case is included in Appendix B.

3.2 Observational results

The extragalactic IRB is very hard to measure directly, as there is a lot of contamination from foreground sources, in particular interplanetary dust in the solar system, as well as interstellar dust and other emissions from the Galaxy. To get an accurate estimate of the IRB, one needs to find models for each of these emissions and remove them from the observed spectrum.

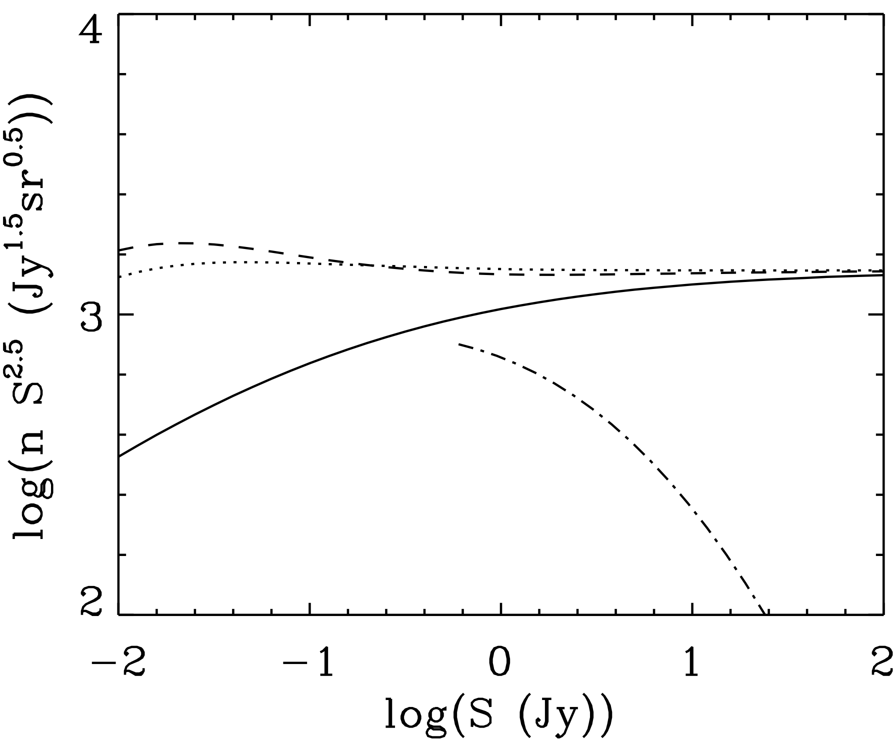

Figure 3.2: Differential sourcecounts. Solid line is no evolution, dotted line is pure luminosity evolution (Eq. (3.8)), dashed line is evolution from Condon [19], and dot-dash line is the luminosity function from Saunders et al. [20].

An important recent result comes from Puget et al. [25], using data obtained from the Far Infrared Absolute Spectrometer (FIRAS) on board COBE. Their technique involved removing model contributions from these foreground sources, as well as the microwave background (since these measurement were made in a region of the spectrum dominated by the CMB). The result is a spectrum that roughly follows a power law of

$$\nu I_\nu \simeq 3.45 \times 10^{-9} \left(\frac{\lambda}{400\mu\text{m}}\right)^{-3} \text{W m}^{-2}\text{ sr}^{-1}$$

for $400\mu\text{m} \leq \lambda \leq 1000\mu\text{m}$. For I_ν in terms of frequency, this becomes

$$I_\nu \simeq 4.5 \times 10^{-21} \left(\frac{\nu}{7.5 \times 10^{11}\text{Hz}}\right)^{2} \text{W m}^{-2}\text{ Hz}^{-1}\text{ sr}^{-1}$$

for $7.5 \times 10^{11}\text{Hz} \geq \nu \geq 3 \times 10^{11}\text{Hz}$.

Another recent result from COBE, this time from the Diffuse Infrared Background Explorer (DIRBE), is that from Hauser [27], quoted in Kashlinsky et al. [26]. The residual results from [27], that is, the measurements after some model of foreground emission has been removed, are summarised in the following table, where the values given are the upper limits of the residuals (i.e. the values with the least amount of foreground emission removed).

λ (μm)	ν (Hz)	I_ν(W m^{-2} Hz^{-1} sr^{-1})
1.25	2.4×10^{14}	4.3×10^{-22}
2.2	1.4×10^{14}	1.9×10^{-22}
3.5	8.6×10^{13}	3.1×10^{-22}

These points are shown on each of the plots in Fig. 3.3, as is the power law from [25].

3.3 Theoretical Predictions

Because of the difficulty in observing the IRB directly, a lot of work has been done to find suitable models for it. In recent years, there have been a number of predictions made regarding the IRB over a range of frequencies. In this section, I review several of these and compare their predictions with each other.

A quite useful result is that of Macminn and Primack [12], who give a comprehensive prediction covering wavelengths from 0.1μm to 1000μm (3×10^{15} Hz to 3×10^{11} Hz). Their prediction is based on different models of galaxy formation: either with cold dark matter (CDM) (consisting of a universe of 90% cold dark matter) or a mixture of cold and hot dark matter (CHDM) (60% CDM and 30% massive neutrinos). The other 10% in each case is the normal, baryonic matter.

Besides the composition, the main difference between the two models is when the era of star formation (redshift $z_{\rm f}$) takes place, as this is the main source of the infrared background. In the CDM models, galaxies form earlier, at formation redshifts of $1 < z_{\rm f} < 3$, while in the CHDM models, they form later, $0.2 < z_{\rm f} < 1$. Both sets of models represent average properties of starburst and other infrared luminous galaxies, as well as normal galaxies. Starburst galaxies are those whose output is dominated by large numbers of young, massive, hot stars. Dust in the galaxies contributes to the infrared emission by absorbing radiation and re-emitting in the infrared. (See, for example, Calzetti [21], or the recent review by Morwood [22].) Sources not included in the modelling would either be at high redshift (in which case there is no known population to identify them with), or would be intrinsically dim (which would produce little effect to the overall background). They do caution, however, that they have not considered more "exotic" mechanisms for producing the IRB, so the lowest of their curves should be taken as the lower limit to the IRB. In Fig 3.3, I have shown the upper and lower envelopes of the set of curves.

De Zotti et al. [13] and Franceschini et al. [14] both give predictions for the IRB in the far infrared (long wavelengths or low frequencies). The predictions from [13] bound what they term a "conservative allowed region", that is, a region where the IRB is most likely to be found, since the lower curve assumes no evolution and is inconsistent with counts at 60μm, and the lower curve assumes a rate of evolution that is inconsistent with the low number of faint high redshift galaxies observed by IRAS. The curve plotted on Fig 3.3 from [14] is the expected minimal contribution from galaxies, assuming no evolution, and is therefore to be taken as a lower limit. Both of these papers also give predictions for the integrated emission of starlight from galaxies in the near infrared ($1-10\mu$m).

Another useful prediction is from Väisänen [15], this time in near infrared to optical wavelengths. He models a number of different classes of galaxies, taking into account different evolutionary models. I have included the upper bound of his predictions (taken from Fig.7 of [15]).

Finally, a recent paper by Stecker and De Jager [23] includes two theoretical predictions, based on the models of Franceschini et al. (1994) [24] and normalised to fit the observational data from Puget et al. [25].

These various models are shown on Fig. 3.3, in comparison with the observational constraints from Puget et al. [25] and Hauser [27]. Also shown are the results of my calculation of the IRB at 60μm. These points correspond to, from the top: evolution functions from Condon [19]; pure luminosity evolution according to Eq. (3.8); no evolution ($f(z) = g(z) = 1$); and the luminosity function and evolution from Saunders et al. [20]. The dashed line in each plot is the CMB, discussed briefly in the next section.

3.4 Microwave Background

As well as the IRB, the other background radiation field of interest for gamma ray astronomy is the cosmic microwave background (CMB). This is the relic photon field that is left over from the big bang. The photons have been travelling through space since the surface of last scattering at redshift $z \sim 1100$.

It has been shown by the FIRAS instrument on board COBE (Fixsen et al. [30]) that the microwave spectrum is almost an exact blackbody, with deviations of less than 50 parts per million, with a temperature of $T = 2.728 \pm 0.004$ K. Since it is a blackbody spectrum, its intensity is given by the Planck formula

$$I_\nu = \frac{2h\nu^3}{c^2}\frac{1}{\exp(\frac{h\nu}{kT}) - 1}$$

where h is Planck's constant, and k is the Boltzmann constant. The blackbody spectrum is shown on each of the plots in Fig. 3.3, demonstrating how the intensity of the CMB is far greater than that of the IRB.

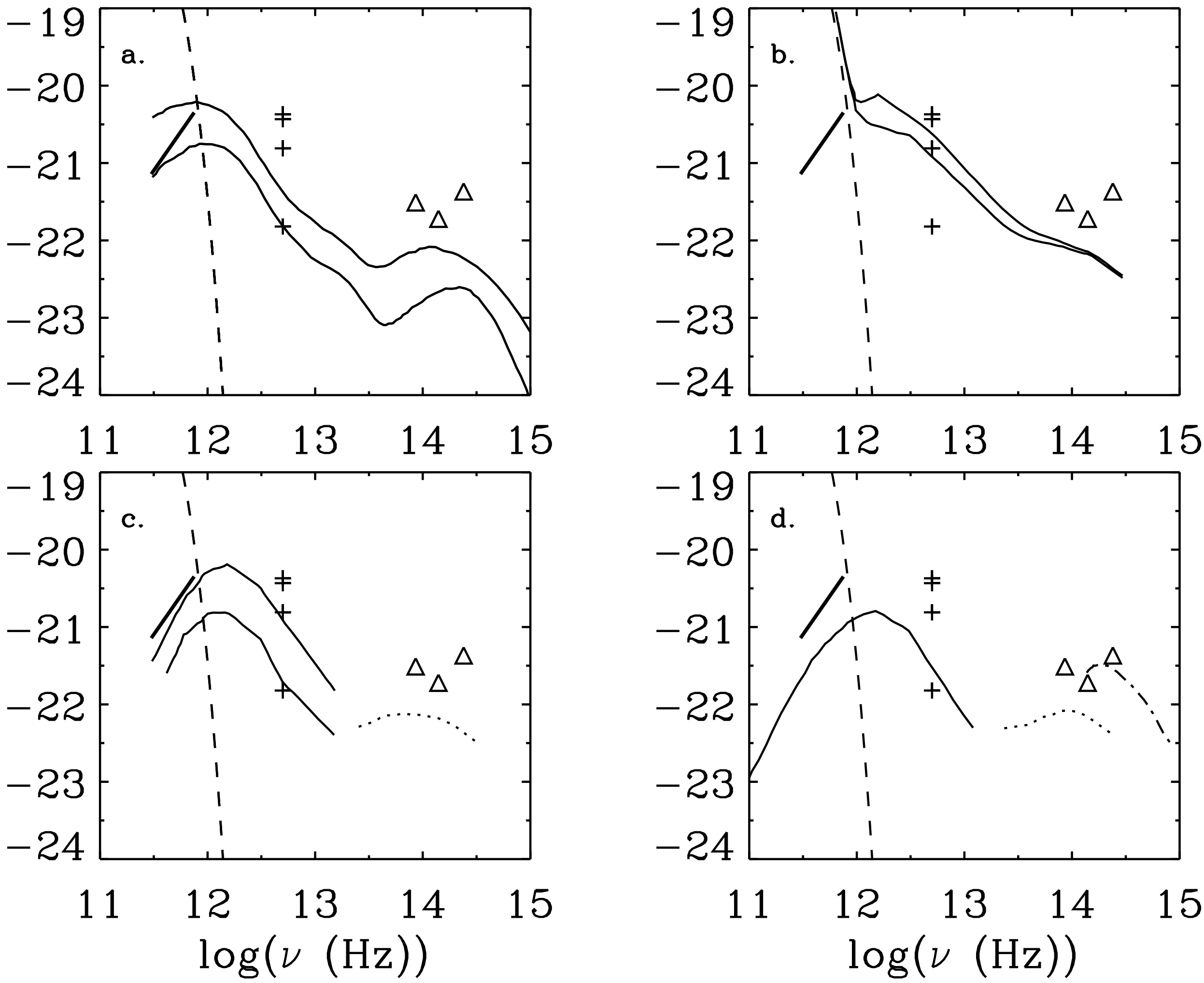

Figure 3.3: Plot of infrared background intensity predictions. The vertical axes in each case are $\log(I_\nu)$, where I_ν is in units of W m^{-2} Hz^{-1} sr^{-1}. Each plot shows the power law from the observations of Puget et al. [25] (thick line), the upper limits of the residuals from the observations from Hauser [27] (triangles), and the results from my program, calculating the background at 60μm (+ signs). Also shown is the microwave background (dashed line). **a.** Upper and lower envelopes of the curves from Macminn and Primack [12]. **b.** Upper and lower curves are curves 1. and 2. repssectively from Stecker and de Jager [23]. The curves are shown continuing into the region dominated by the CMB. **c.** The upper and lower solid curves are curves c) and a) respectively from DeZotti et al. [13]. The dotted curve is curve d) from the same paper. **d.** The solid curve is curve G2 from Franceschini et al. [14], while the dotted curve is curve G3 from the same paper. The dot-dash curve is the upper envelope from Väisänen [15].

Chapter 4

Interactions

4.1 Introduction

When considering the propagation of gamma-rays through an extragalactic background radiation field (either infra-red or microwave), there are two main interactions that will alter the spectrum of the gamma-rays: photon-photon pair production, where the gamma-ray interacts with a soft (infrared or microwave) photon to produce an electron-positron pair; and inverse compton scattering, where an electron produced via pair production collides with a soft photon, increasing its energy.

These processes will alter the shape of the gamma-ray spectrum emitted from such sources discused in the first chapter. Pair-production in the soft photon field will decrease the spectrum, whereas the inverse compton scattering by relativistic electrons can increase the energy of the soft photons up to gamma-ray energies.

4.2 Cross sections

The cross section, σ, is a key quantity in the analysis of such interactions. It is a measure of the probability of the interaction occuring, for given values of the initial energies and momenta. The units of σ are those of area, e.g. cm^2, so σ gives the effective cross sectional area of the interaction. Also of use is the differential cross section $d\sigma/d\Omega$, which is the cross section for the interaction given that the final momenta lie in a differential range of solid angle $d\Omega$.

4.2.1 Photon-photon pair production cross sections

Photon-photon pair production occurs when two photons interact to produce an electron-positron pair: $\gamma + \gamma \rightarrow e^+ + e^-$. Throughout this thesis, there will be no distinction made between the e^+ and e^- particles, and the term "electron" will be used to refer to both particles. The interaction is considered in the centre of momentum (CM) frame, where the two photons have equal energy. By energy conservation, the energies of the electrons in the CM frame are the same as those of the photons. The differential cross section for such a process can be shown (a full derivation is given in Jauch and Rohrlich [29]) to be

$$\frac{d\sigma_{\gamma\gamma}}{d\cos\alpha} = \frac{\pi r_0^2}{2}\beta\left(\frac{m_e c^2}{E_\gamma}\right)\frac{1-\beta^4\cos^4\alpha + 2(m_e c^2/E_\gamma)^2\beta^2\sin^2\alpha}{(1-\beta^2\cos^2\alpha)^2}. \tag{4.1}$$

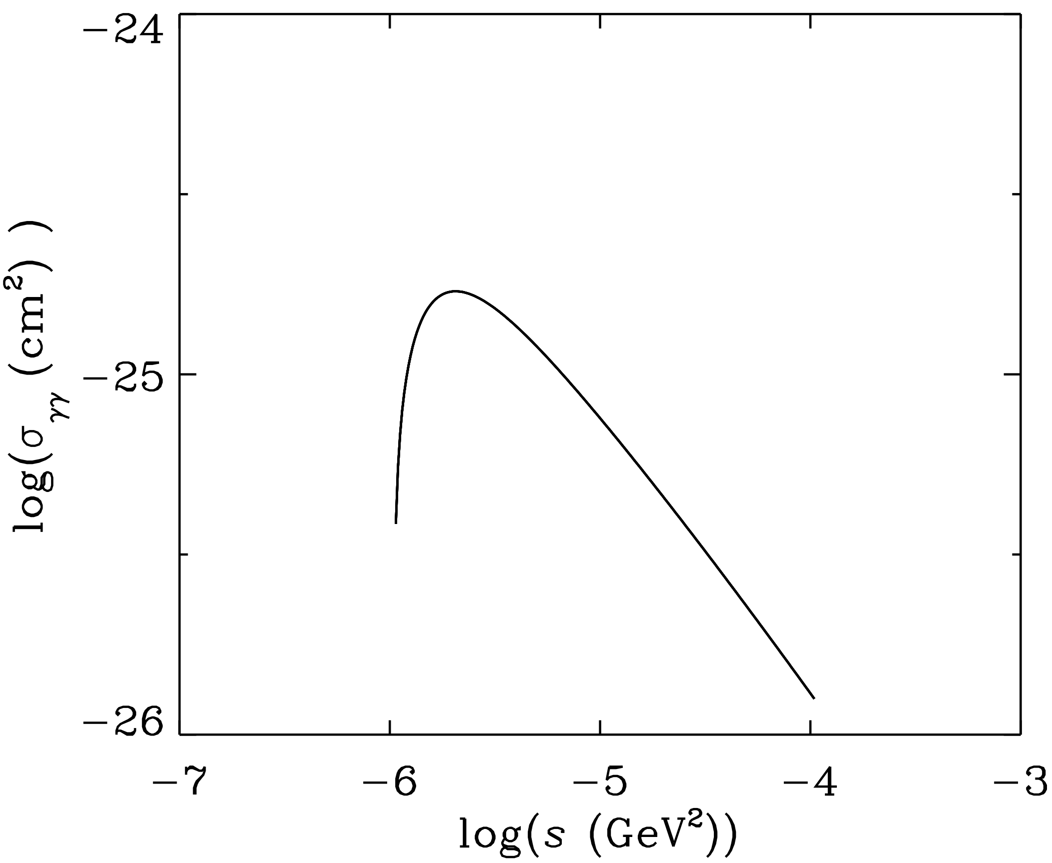

Figure 4.1: Total cross section for photon-photon pair production vs. s.

Here, $m_e c^2$ is the electron rest mass energy, E_γ is the energy of one of the photons in the CM frame, r_0 is the classical electron radius with the value $r_0 = 2.82 \times 10^{-13}$ cm, α is the scattering angle, that is, the angle the electron directions make with respect to the photon directions, and β is defined by

$$\beta = \sqrt{1 - \left(\frac{m_e c^2}{E_\gamma}\right)^2} = \sqrt{1 - \left(\frac{4m_e^2 c^4}{s}\right)}$$

where $s = (2E_\gamma)^2$, the total CM frame energy squared, and $m_e c^2$ is the rest mass energy of the electron, with the value $m_e c^2 = 5.11 \times 10^{-4}$ GeV. Note that since Eq. (4.1) is independent of azimuthal angle ϕ, the solid angle is given by $d\Omega = d\phi\, d\cos\alpha = 2\pi\; d\cos\alpha$, and so

$$\frac{d\sigma_{\gamma\gamma}}{d\Omega} = 2\pi \frac{d\sigma_{\gamma\gamma}}{d\cos\alpha}$$

This can be integrated to give the total cross section for photon-photon pair production:

$$\sigma_{\gamma\gamma} = \frac{\pi r_0^2}{2}(1-\beta^2)\left[(3-\beta^4)\ln\frac{1+\beta}{1-\beta} - 2\beta(1-\beta^2)\right] \tag{4.2}$$

As seen in Fig 4.1, $\sigma_{\gamma\gamma}$ increases with s from the threshold value of $s = (2mc^2)^2$ to a maximum, then decreases as the energy increases.

4.2.2 Inverse compton scattering cross sections

Inverse compton scattering occurs when a relativistic electron collides with a photon, increasing its energy. This is different to the usual case of compton scattering, where energy is transfered from the photon to the electron. In this case, the final photon energy ϵ_1, in terms of ϵ, the initial energy, and α, the angle through which the photon is scattered, is

$$\epsilon_1 = \frac{\epsilon}{1 + \frac{\epsilon}{m_e c^2}(1 - \cos\alpha)}.$$

This equation applies to the case of an initially stationary electron. Thus, inverse compton scattering can be considered by boosting from the LAB frame to the electron's rest frame (ERF), calculating the change in energy of the photon by the above equation, then boosting back to the LAB frame.

The differential cross section can be calculated (e.g. in [29]) to be (in the ERF)

$$\frac{d\sigma_{\gamma e}}{d\Omega} = \frac{r_0^2}{2}\left(\frac{\epsilon_1}{\epsilon}\right)^2\left(\frac{\epsilon_1}{\epsilon} + \frac{\epsilon}{\epsilon_1} - \sin^2\alpha\right) \tag{4.3}$$

where ϵ_1 is given by the equation above. This expression can be integrated to give the total cross section (which is independent of the choice of frame) as follows

$$\sigma_{\gamma e} = \frac{3}{4}\sigma_{\mathrm{T}}\left\{\frac{1+x}{x^3}\left[\frac{2x(1+x)}{1+2x} - \ln(1+2x)\right] + \frac{\ln(1+2x)}{2x} - \frac{1+3x}{(1+2x)^2}\right\} \tag{4.4}$$

where $x \equiv \epsilon/mc^2$, and σ_{T} is the Thomson cross section, $\sigma_{\mathrm{T}} = 0.655 \times 10^{-24}$ cm^2. This is the classical value for scattering of low energy photons off electrons, as first done by J.J.Thomson.

For small energies, $\epsilon \ll m_e c^2$, there is negligible change in the photon energy, $\epsilon_1 \simeq \epsilon$ or $\epsilon_1/\epsilon \simeq 1$, so the differential cross section becomes

$$\frac{d\sigma_{\gamma e}}{d\Omega} \simeq \frac{r_0^2}{2}(2 - \sin^2\alpha) = \frac{r_0^2}{2}(1 + \cos^2\alpha).$$

This can be integrated, using $d\Omega = 2\pi d\cos\alpha$,

$$\begin{aligned} \sigma &= \pi r_0^2 \int_{-1}^{1}(1+\cos^2\alpha)d\cos\alpha \\ &= \pi r_0^2\left[\cos\alpha + \frac{1}{3}\cos^3\alpha\right]_{\cos\alpha=-1}^{\cos\alpha=1} \\ &= \frac{8\pi}{3}r_0^2 = \sigma_{\mathrm{T}} \end{aligned}$$

As the energy of the photon decreases, it moves into this classical regime, and the cross section becomes constant, as shown in Fig 4.2 (here the cross section is plotted against s, the total CM frame energy squared, which is directly related to the photon energy in the ERF by a Lorentz boost). As the energy increases, the cross section decreases from its classical value.

4.3 Interaction lengths

An important quantity to know when dealing with these interactions over large (e.g. intergalactic) distances is the mean interaction length, or mean free path. This is the

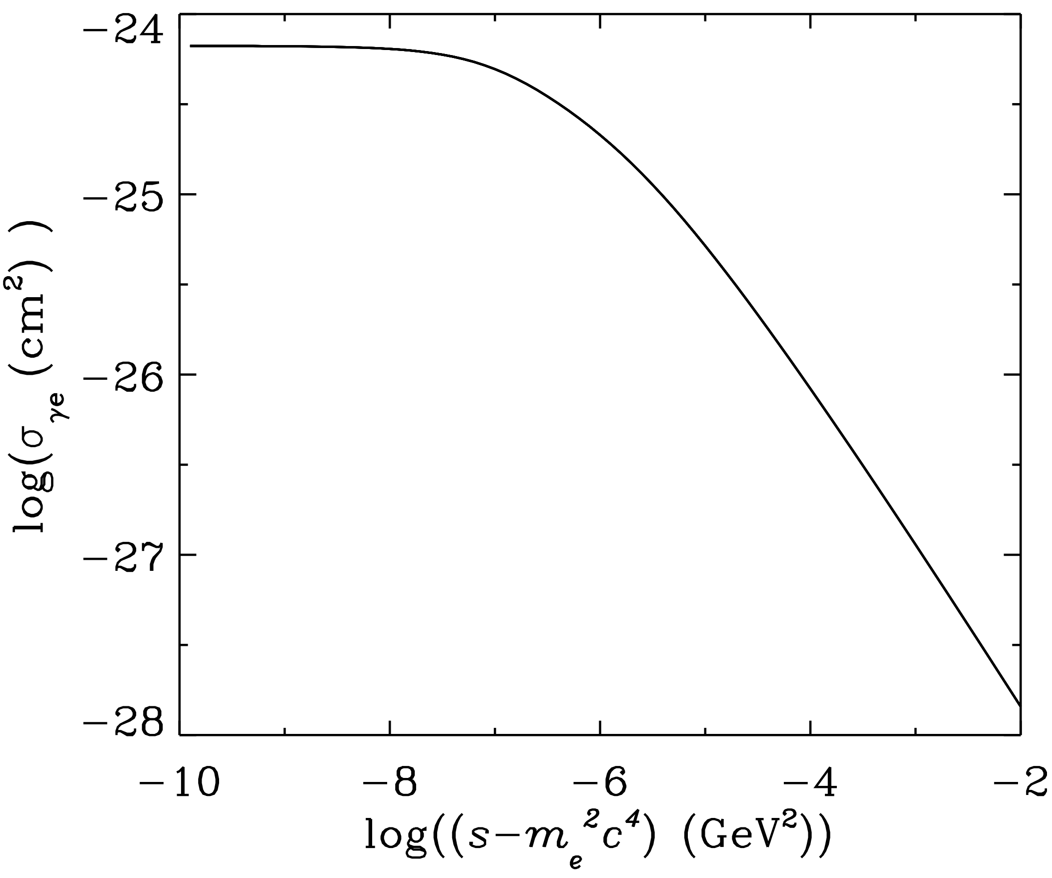

Figure 4.2: Total cross section for inverse compton scattering vs. s.

average distance an incident particle (photon, electron, or otherwise) will travel before undergoing an interaction. The mean free path of a particle of energy E through a radiation field is denoted by $\lambda(E)$, and is given in general by the following integral

$$\frac{1}{\lambda(E)} = \frac{1}{8\beta E^2} \int_{\epsilon_{\min}}^{\infty} \frac{n(\epsilon)}{\epsilon^2} \int_{s_{\min}}^{s_{\max}} \sigma(s)(s - m^2c^4)\; ds\; d\epsilon \tag{4.5}$$

where: the incident particle has mass m and velocity βc; $n(\epsilon)$ is the differential number density of photons of energy ϵ in the radiation field; s is the CM frame energy squared, given by

$$s = m^2c^4 + 2\epsilon E(1 - \cos\theta) \tag{4.6}$$

with θ the angle between the directions of the incident particle and the soft photon (i.e. the photon from the radiation field); and $\sigma(s)$ is the total cross section for the interaction in question, as a function of s. This equation applies for all types of particles incident on a radiation field, be they photons, electrons, protons, or otherwise. Of course, I shall only consider gamma-ray photons and electrons.

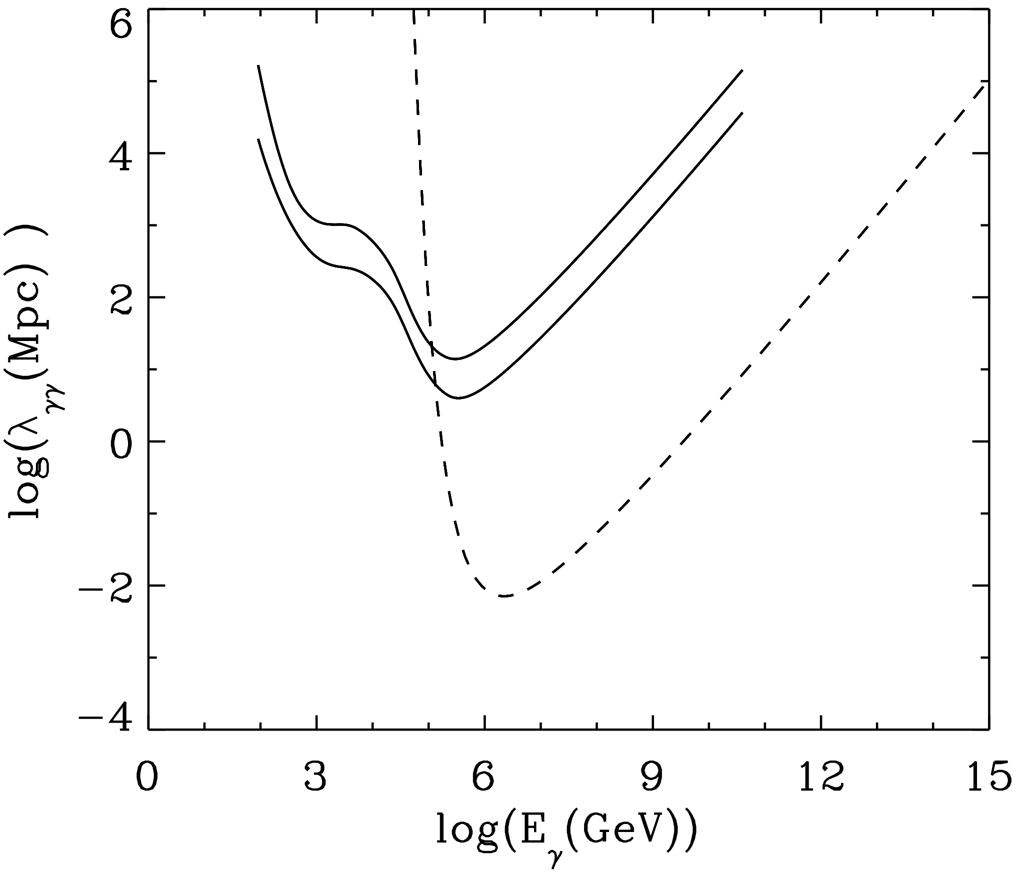

Figure 4.3: Mean interaction lengths for gamma rays against pair production in the microwave and infra-red backgrounds. The dashed line gives the mean interaction length in the cosmic microwave background. The lower and upper dashed lines give the mean interaction lengths using the upper and lower envelopes respectively of the IRB predictions from Macminn and Primack [12].

4.3.1 Interaction lengths for pair production

For gamma-rays undergoing photon-photon pair production, $m = 0$ and $\beta = 1$, so the integral becomes

$$\frac{1}{\lambda_{\gamma\gamma}(E)} = \frac{1}{8E^2}\int_{\epsilon_{\rm min}}^{\infty}\frac{n(\epsilon)}{\epsilon^2}\int_{s_{\rm min}}^{s_{\rm max}}\sigma_{\gamma\gamma}(s)s\ ds\ d\epsilon \tag{4.7}$$

where $s = 2\epsilon E(1-\cos\theta)$, $s_{\rm max}(\epsilon, E) = 4\epsilon E$ and $s_{\rm min} = (2m_ec^2)^2$, since there are two electrons produced in the CM frame, and they each must have an energy of at least their rest mass, m_ec^2. The cross section, $\sigma_{\gamma\gamma}$, is the total cross section for photon-photon pair production, and is given by Eq. (4.2).

Since $s_{\rm min} = (2m_ec^2)^2$, a value for $\epsilon_{\rm min}$ can be obtained. The lowest energy collision will be a head on one ($\theta = \pi$), involving the lowest energy photon, of energy $\epsilon_{\rm min}$. Thus

$$(2m_ec^2)^2 = 4E\epsilon_{\rm min}$$

$$\epsilon_{\rm min} = \frac{(m_ec^2)^2}{E}.$$

The differential number density $n(\epsilon)$ is given by

$$n(\epsilon) = \frac{4\pi}{hc}\frac{I_\nu}{h\nu}$$

where I_ν is the specific intensity of the radiation field at frequency $\nu = \epsilon/h$. Thus, given an intensity spectrum of a radiation field, such as the blackbody spectrum of the CMB or one of the IRB spectra discussed in Section 3.3, one can calculate the mean free path of a gamma ray through the field against photon-photon pair production interactions.

Firstly, consider the CMB, which is a blackbody spectrum of temperature 2.728 K [30]. The specific intensity of a blackbody spectrum of temperature T is given in terms of ν by

$$I_\nu = \frac{2h\nu^3}{c^2}\frac{1}{\exp(\frac{h\nu}{kT}) - 1}$$

where k is the Boltzmann constant. Since $\epsilon = h\nu$, this can be rewritten in terms of ϵ.

$$I_\nu = \frac{2\epsilon^3}{h^2c^2}\frac{1}{\exp(\frac{\epsilon}{kT}) - 1}$$

Hence, one gets the expression for the differential number density of CMB photons as a function of energy:

$$n(\epsilon) = \frac{8\pi}{h^3c^3}\frac{\epsilon^2}{\exp(\frac{\epsilon}{kT}) - 1} \tag{4.8}$$

This expression can then be used in Eq. (4.7) to calculate exactly the mean free path of gamma rays through the CMB.

For the IRB, such as that calculated in [12], $n(\epsilon)$ is calculated directly from the prediction of $I_\nu(\nu)$. In my case, this involves digitising the data from the plot in the relevant paper, to form a series of discrete data points. Then, in calculating the integral numerically, I interpolate between the data points to get the necessary values of I_ν. In Fig 4.3, I have included the CMB along with the results from the envelope curves of [12]. Obviously, below a gamma-ray energy of about 10^5 GeV, the mean interaction length in the IRB is much less than that in the CMB, meaning the gamma-ray will interact with an infra-red photon, which is of higher energy than a microwave photon. Above about 10^5 GeV, the opposite is true, with the gamma-ray interacting primarily with the CMB.

4.3.2 Interaction lengths for inverse compton scattering

For inverse compton scattering, the incident particle is an electron, which is massive ($m_e \neq 0$) and has $\beta < 1$. Thus, we can use Eq. (4.5) without alteration, except to define the integration limits. Since $s = m_e^2c^4 + 2\epsilon E(1 - \beta\cos\theta)$, the maximum and minimum values of s for given values of E and ϵ are

$$s_{\max} = m_e^2c^4 + 2\epsilon E(1 + \beta)$$

$$\text{and} \quad s_{\min} = m_e^2c^4 + 2\epsilon E(1 - \beta)$$

respectively. In practice, since the electrons being considered have energies ≥ 100 GeV, β is very close to 1, so $s_{\min} \simeq m_e^2c^4$. Also, there is no threshold value for ϵ for inverse compton scattering (unlike pair production, where there needs to be enough energy to

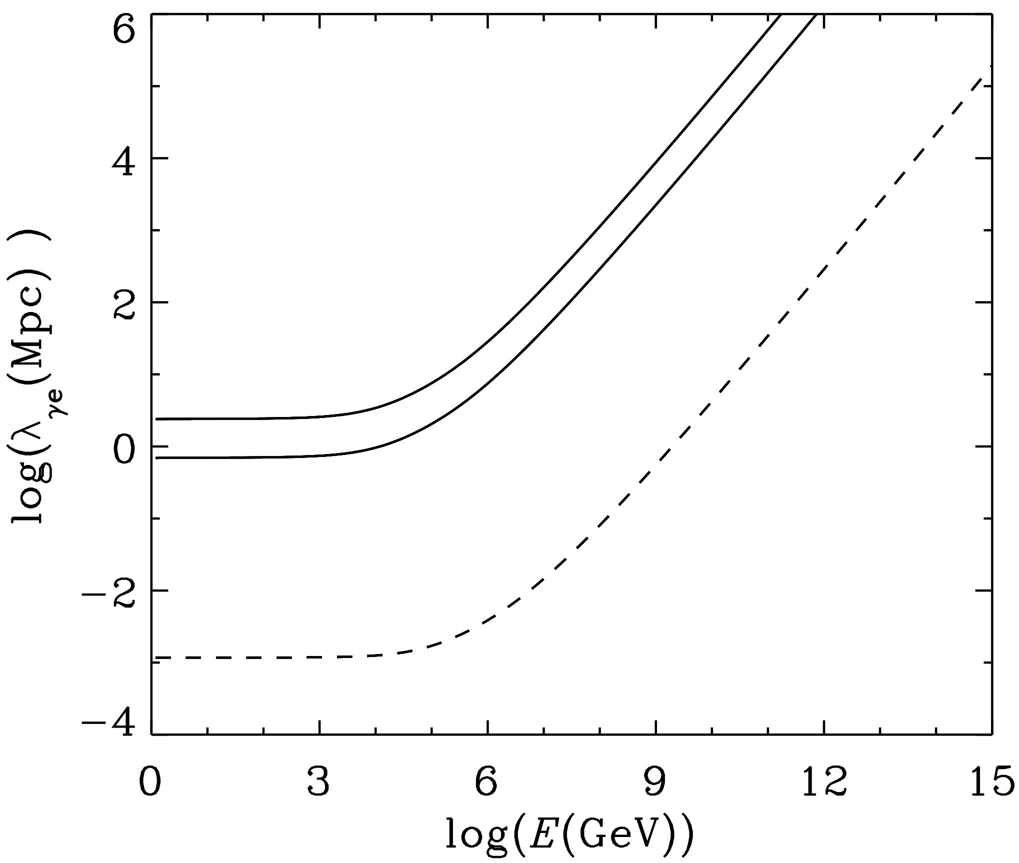

Figure 4.4: Mean interaction lengths for electrons against inverse compton scattering in the microwave and infra-red backgrounds. The dashed line gives the mean interaction length in the cosmic microwave background. The lower and upper solid lines give the mean interaction lengths using the upper and lower envelopes respectively of the IRB predictions from Macminn and Primack [12].

create at least two electron rest masses), so $\epsilon_{\min} = 0$. So for an incident electron with energy E, travelling at velocity βc, the mean free path $\lambda_{\gamma e}(E)$ is given by

$$\frac{1}{\lambda_{\gamma e}(E)} = \frac{1}{8\beta E^2} \int_0^\infty \frac{n(\epsilon)}{\epsilon^2} \int_{s_{\min}}^{s_{\max}} \sigma_{\gamma e}(s)(s - m_e^2 c^4)\ ds\ d\epsilon \tag{4.9}$$

where $\sigma_{\gamma e}$ is the total cross section for inverse compton scattering, given by Eq (4.4). The calculations for $n(\epsilon)$ are as for pair production, so the mean free path can be calculated for both the IRB and the CMB in the same way. However, one notices from Fig 4.4 that the mean free path in the CMB is around three orders of magnitude less than in the IRB, so inverse compton scattering in the IRB can be neglected. That is, a relativistic electron will interact with a microwave photon far earlier than with an infra-red photon.

Note from Fig 4.4 that below about 1000 GeV, λ is constant. This is because, for low energies, the compton scattering cross section $\sigma_{\gamma e}$ is given by the Thomson cross section, $\sigma_{\mathrm{T}} = 0.655 \times 10^{-24}$ cm^2. The mean free path equation, Eq. (4.9), can be written as

$$\frac{1}{\lambda_{\gamma e}(E)} = \int_0^\infty n(\epsilon) \int_{-1}^{1} \frac{\sigma_{\gamma e}(s)}{2}(1 - \beta\cos\theta)\ d(\cos\theta)\ d\epsilon,$$

and if $\sigma = \sigma_{\mathrm{T}}$, then

$$\begin{aligned}\frac{1}{\lambda_{\gamma e}(E)} &= \frac{\sigma_{\mathrm{T}}}{2}\int_0^\infty n(\epsilon)\int_{-1}^{1}(1-\beta\cos\theta)\ d(\cos\theta)\ d\epsilon \\ &= \sigma_{\mathrm{T}}\int_0^\infty n(\epsilon)\ d\epsilon.\end{aligned}$$

Hence the value of λ at low energies is completely determined by the differential photon density. If the exact solution for the blackbody photon density, Eq. (4.8), is used, a value for the mean free path at low energies can be obtained:

$$\frac{1}{\lambda_{\gamma e}(E)} = \frac{16\pi\sigma_{\mathrm{T}}}{h^3c^3}\ (kT)^3\zeta(3),$$

where $\zeta(3) \approx 1.202057$, and k is the Boltzmann constant, with the value $k = 8.617 \times 10^{-14}$ GeV K^{-1}. Evaluating this expression gives the value of $\lambda_{\gamma e}(E) = 3.624 \times 10^{21}$ cm = 1.174 kpc

4.4 Geometry of Interactions

This section is concerned with the actual interaction itself. It looks at the directions of the particles involved, the lorentz transformations needed to get from one frame to another, and how the energies of the final particles are computed. However, the techniques used to calculate quantities such as the initial soft photon energy, the angle of incidence and the scattering angle will be discussed in the following chapter.

4.4.1 Pair production

First consider the photon-photon pair production interaction. A high energy photon (i.e. a gamma-ray) of energy E interacts with a lower-energy (or soft) photon of energy ϵ, which is travelling at an angle θ to the direction of propagation of the gamma-ray. Such a setup is shown in Fig 4.5, where I follow the method used by Protheroe [31]. This frame is called the LAB frame, and this is the frame in which the gamma-rays will be observed, so the final energies of all particles need to be calculated in this frame. However, the interaction needs to be considered in the CM frame, where the two photons have equal energy and travel in opposite directions.

To get to the CM frame, you need to apply a boost at an angle ϕ to the gamma-ray direction (as shown in Fig 4.5). This angle can be calculated by equating the momenta in the LAB frame perpendicular to the boost direction:

$$E\sin\phi = \epsilon\sin(\theta-\phi) = \epsilon\sin\theta\cos\phi - \epsilon\cos\theta\sin\phi$$

$$(E+\epsilon\cos\theta)\sin\phi = \epsilon\sin\theta\cos\phi$$

$$\phi = \tan^{-1}\left[\frac{\epsilon\sin\theta}{(E+\epsilon\cos\theta)}\right] \tag{4.10}$$

The velocity of the boost is β^*c, where β^* can be found by setting the momenta in the CM frame to be equal and opposite. The momenta in the CM frame are given in terms of the LAB frame energies and angles by: (setting $c = 1$)

$$p_1' = \gamma^*(E\cos\phi - \beta^*E)$$

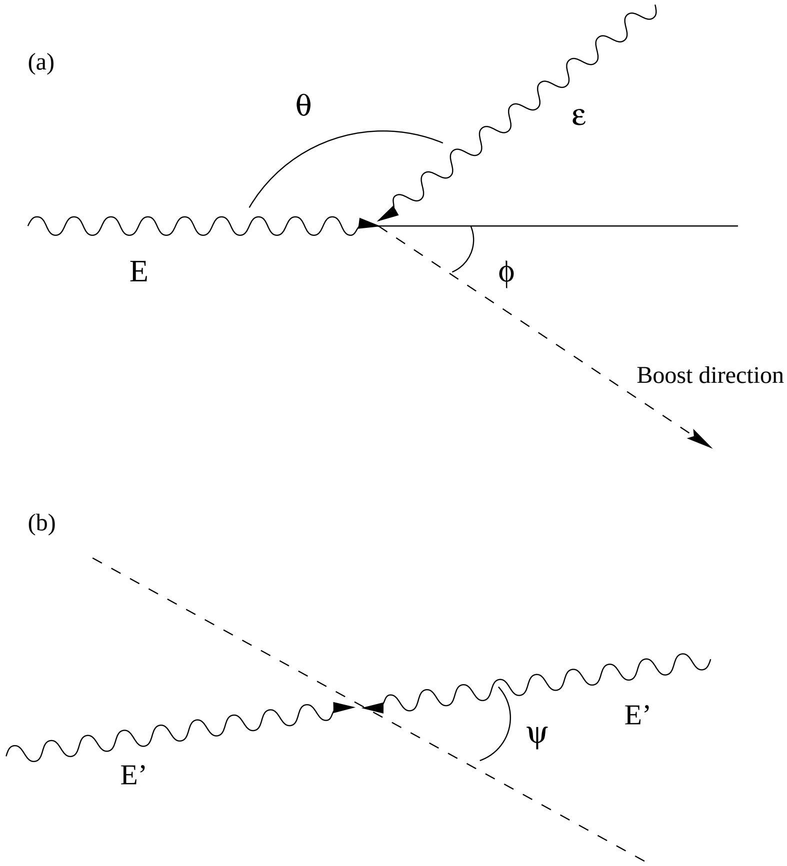

Figure 4.5: (**a**) LAB frame: Gamma ray of energy E and soft photon of energy ϵ, showing direction of boost needed to get to CM frame. (**b**) CM frame: Photon directions, as well as boost direction. Diagram taken from Protheroe [31].

$$p_2' = \gamma^*(\epsilon\cos(\theta-\phi) - \beta^*\epsilon)$$

where p_1' and p_2' are the momenta of the gamma ray and the soft photon respectively in the boost direction in the CM frame, and

$$\gamma^* = (1-\beta^{*2})^{-1/2}.$$

By setting $p_1' = -p_2'$, as must be the case in the CM frame, we get

$$\beta^* = \frac{E\cos\phi + \epsilon\cos(\theta-\phi)}{E+\epsilon}. \tag{4.11}$$

In the CM frame, the photons travel in opposite directions, so that they undergo a head-on collision. The angle they make with the boost direction is Ψ (see Fig 4.5), given by the aberration formulae:

$$\sin\Psi = \frac{\sin\phi}{\gamma^*(1-\beta^*\cos\phi)}, \quad \cos\Psi = \frac{\cos\phi - \beta^*}{1-\beta^*\cos\phi}$$

So that we have

$$\Psi = \tan^{-1}\left[\frac{sin\phi}{\gamma^*(\cos\phi-\beta^*)}\right] \tag{4.12}$$

The energies of the photons in the CM frame are calculated using conservation of 4-momentum. Let k_1 and k_2 denote the 4-momenta of the gamma-ray and the soft photon respectively in the LAB frame, and k_1' and k_2' the respective 4-momenta in the CM frame. Then, by conservation of 4-momentum,

$$(k_1 + k_2)^2 = (k_1' + k_2')^2.$$

Since $k \cdot k = 0$ for photons, we have

$$k_1 \cdot k_2 = k_1' \cdot k_2'$$

$$E\epsilon(1 - \cos\theta) = E'\epsilon'(1 - \cos\theta')$$

where a $'$ means the quantity is measured in the CM frame. This frame is defined by requiring $E' = \epsilon'$ and $\theta' = \pi$. So, the energy of each photon in the CM frame is given by

$$E' = \sqrt{\frac{1}{2}E\epsilon(1 - \cos\theta)} \tag{4.13}$$

or, in terms of s, the total CM frame energy squared,

$$E' = \frac{\sqrt{s}}{2} \tag{4.14}$$

Again by conservation of 4-momentum, the electrons will be emitted each with an energy equal to E'. However, to calculate their energies in the LAB frame, the direction that the electrons are travelling needs to be known, in particular, momentum of each electron in the direction of the boost.

To do this, consider the components of the momenta of the particles. Let the plane that the two photons lie in be the x-y plane, and choose the x-axis to be in the direction of the boost. Then the momenta of the gamma-ray and soft photon in the LAB frame are given respectively by

$$\hat{k}_1 = (\cos\phi, \sin\phi, 0)$$

$$\hat{k}_2 = (\cos(\theta - \phi), sin(\theta - \phi), 0)$$

and in the CM frame they are

$$\hat{k}_1' = (\cos\Psi, \sin\Psi, 0)$$

$$\hat{k}_2' = (-\cos\Psi, -\sin\Psi, 0)$$

where Ψ is given by Eq. (4.12).

Now define new axes $\hat{\imath}, \hat{\jmath}, \hat{k}$ defined in terms of the usual cartesian axes $\hat{x}, \hat{y}, \hat{z}$ by

$$\hat{\imath} = \hat{k}_1' = (\cos\Psi, \sin\Psi, 0)$$

$$\hat{\jmath} = \frac{\hat{y} \times \hat{\imath}}{|\hat{y} \times \hat{\imath}|} = (0, 0, -1)$$

$$\hat{k} = \hat{\imath} \times \hat{\jmath} = (-\sin\Psi, \cos\Psi, 0)$$

This way, the photon trajectories lie on the $\hat{\imath}$ axis. The electron, when emitted, is scattered by an angle α from the direction of the photon, so that the momentum vector of the electron lies on a cone centred on the $\hat{\imath}$ axis, with half-angle α. To determine where on this cone the vector lies, another parameter is needed. This is the so-called azimuthal angle, δ, measured around the "base" of the cone, starting with $\delta = 0$ when the momentum perpendicular to the $\hat{i}$ axis is in the $\hat{j}$ direction. Both of these angles - the scattering angle and the azimuthal angle - need to be calculated and/or sampled. The techniques for this are discussed in the next chapter.

Thus, $\hat{p}_1'$ can be written as

$$\hat{p}_1' = \cos\alpha\ \hat{i} + \sin\alpha\cos\delta\ \hat{j} + \sin\alpha\sin\delta\ \hat{k}$$

or, in terms of the $\hat{x}, \hat{y}, \hat{z}$ coordinates

$$\hat{p}_1' = (\cos\alpha\cos\Psi - \sin\alpha\cos\delta\sin\Psi,\ \cos\alpha\sin\Psi + \sin\alpha\cos\delta\cos\Psi,\ -\sin\alpha\sin\delta).$$

The other electron has momentum $\hat{p}_2' = -\hat{p}_1'$, since it is emitted in the opposite direction to conserve momentum. The CM frame energy of each of the electrons is given by Eq. (4.13).

To get the energies in the LAB frame, a boost is applied in the opposite direction to the one that changed frames from the LAB to the CM. If p_{1x} denotes the momentum of electron 1 in the $\hat{x}$ direction (i.e. the direction of the boost), then the LAB frame energy of that electron is

$$E_1 = \gamma^*(E' + \beta^* p_{1x} c),$$

so that the energies of the two electrons are given by

$$E_{1,2} = \gamma^*\Big[E' \pm \beta^*(\gamma\beta mc^2)(\cos\alpha\cos\Psi - \sin\alpha\cos\delta\sin\Psi)\Big] \qquad (4.15)$$

where E_1 has a $+$ sign and E_2 has a $-$ sign. The factor of $\gamma\beta mc^2$ comes from the magnitude of the momentum in the CM frame. Since $\hat{p}_1$ is a unit vector, $\mathrm{p}_1\hat{p}_1$ gives the vector $\vec{p}_1$, with magnitude

$$\mathrm{p}_1 = \gamma m v = \gamma m c\beta$$
$$\Rightarrow\ \mathrm{p}_1 c = \gamma\beta mc^2$$

where $v = \beta c$ is the velocity of the electrons in the CM frame, and $\gamma = (1-\beta^2)^{-1/2}$.

4.4.2 Inverse compton scattering

The analysis of the inverse compton scattering interaction is similar to the above. In the LAB frame, a relavtivistic electron with energy E interacts with a soft photon of energy ϵ_1, which is travelling at an angle θ to the direction of the electron, as shown in Fig 4.6. The interaction itself is considered in the electron's rest frame (ERF), where the electron is stationary, and so compton scattering is used. A lorentz boost is applied in the direction of the electron's motion to move from the LAB frame to the ERF, where the speed of the boost is that of the electron in the LAB frame.

To calculate the energy of the scattered photon in the LAB frame, a similar procedure is used to that for pair production. First, take the plane of the electron and photon directions to be the x-y plane, as shown in Fig 4.6. The unit vector of momentum for the soft photon in the LAB frame is thus given by

$$\hat{k}_1 = (\cos\theta, \sin\theta, 0)$$

and in the ERF by

$$\hat{k}_1' = (\cos\theta', \sin\theta', 0),$$

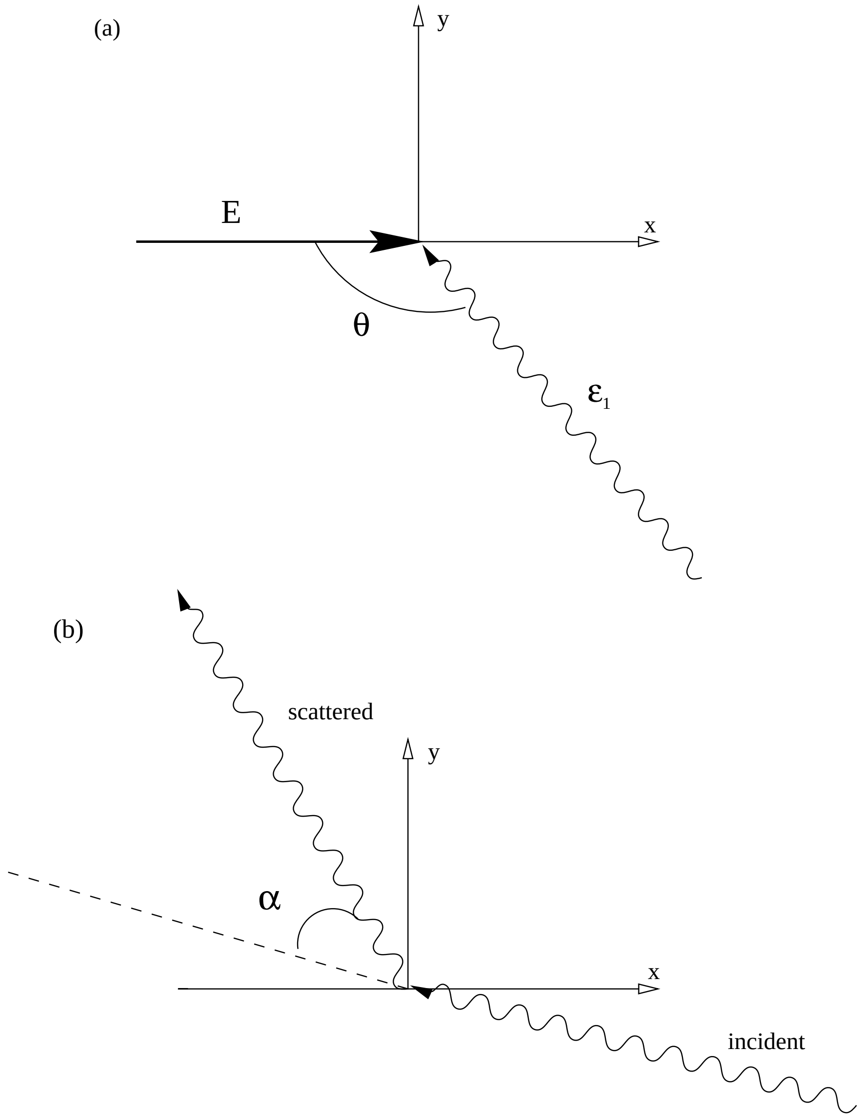

Figure 4.6: (**a**) LAB frame: Electron of energy E and soft photon of energy ϵ_1, with angle of incidence θ. (**b**) ERF frame: Photon directions, before and after scattering, showing scattering angle α.

where, the $'$ means measured in the ERF. The expressions involving θ' come from the aberration formulae

$$\sin\theta' = \frac{\sin\theta}{\gamma(1-\beta\cos\theta)}, \quad \cos\theta' = \frac{\cos\theta-\beta}{1-\beta\cos\theta}$$

where βc is the boost velocity, and $\gamma = (1-\beta^2)^{-1/2}$.

Now, as before, define axes $\hat{\imath}, \hat{\jmath}, \hat{k}$ in terms of the cartesian axes by

$$\hat{\imath} = \hat{k}_1' = (\cos\theta', \sin\theta', 0)$$

$$\hat{\jmath} = \frac{\hat{y}\times\hat{\imath}}{|\hat{y}\times\hat{\imath}|} = (0,0,-1)$$

$$\hat{k} = \hat{\imath}\times\hat{\jmath} = (-\sin\theta', \cos\theta', 0)$$

Then, when the photon is scattered with scattering angle α and azimuthal angle δ (see next chapter for the method of obtaining these angles), it has momentum unit vector in these coordinates of

$$\hat{k}'_2 = \cos\alpha\hat{\imath} + \sin\alpha\cos\delta\hat{\jmath} + \sin\alpha\sin\delta\hat{\jmath},$$

or, in the original $\hat{x}, \hat{y}, \hat{z}$ coordinates,

$$\hat{k}'_2 = (\cos\alpha\cos\theta' - \sin\alpha\cos\delta\sin\theta',\ \cos\alpha\sin\theta' + \sin\alpha\cos\delta\cos\theta',\ -\sin\alpha\sin\delta).$$

This gives the direction of the momentum vector of the scattered photon in the ERF. The magnitude of the momentum is found from the energy of the photons. The energy of the incident photon in the ERF is obtained by a simple lorentz boost

$$\epsilon'_1 = \gamma\epsilon_1(1 - \beta\cos\theta),$$

and the energy of the scattered photon is given by the equation for compton scattering:

$$\epsilon'_2 = \frac{\epsilon'_1}{1 + \frac{\epsilon'_1}{mc^2}(1 - \cos\alpha)}$$

The magnitude of the momentum of the scattered photon in the ERF is then k $= \epsilon'_2/c$.

Given the energy of the scattered photon, and its momentum in the $\hat{x}$-direction (i.e. in the direction of the boost), the energy of the scattered photon is given by

$$\epsilon_2 = \gamma\epsilon'_2\Big[1 + \beta(\cos\alpha\cos\theta' - \sin\alpha\cos\delta\sin\theta')\Big] \tag{4.16}$$

Chapter 5

Monte Carlo methods

5.1 Introduction

In the previous chapter, expressions were derived for the energies of the final particles resulting from pair production and inverse compton scattering. This derivation, however, assumed the knowledge of quantities that were not derived, namely the soft photon energy (ϵ), the angle of interaction (θ), the scattering angle (α), and the azimuthal angle from the scattering (δ). These quantities are each distributed according to their own distribution, from which they need to be sampled in some way to be used in the earlier expressions.

This chapter will discuss these sampling techniques, as well as the approximations I used to speed up the computational process. The sampling techniques discussed, which use random numbers, are known generally as monte carlo methods. These are named after the Monte Carlo casino in Monaco, since the roulette wheel was often used as an early random number generator.

5.2 Interaction length

Before the quantities mentioned above are calculated, one needs to know the interaction length - the distance that the incident particle has travelled before interacting. This has to be sampled from an appropriate distribution.

The interaction length, x, is distributed according to an exponential distribution

$$p(x) = \frac{1}{\lambda} \exp(-x/\lambda) \tag{5.1}$$

where λ is the mean interaction length, as given by Eq. (4.5). To sample from this distribution, the transformation method is used. Let $w(\xi)$ be a uniform distribution of random numbers:

$$w(\xi) = \begin{cases} 1 & 0 \leq \xi \leq 1 \\ 0 & \text{otherwise} \end{cases}$$

where ξ is a random number (or, to use the correct term, a pseudo-random deviate), generated by a suitable pseudo-random generator. In the case of my programs, I used the IMSL library function RNUNF().

Then, x is sampled according to

$$\int_0^x p(x')\ dx' = \int_0^\xi w(\xi')\ d\xi' = \xi.$$

In the case of the above exponential distribution,

$$\int_0^x \frac{1}{\lambda}\exp(-x'/\lambda) = \xi$$
$$\Big[-\exp(-x'/\lambda)\Big]_0^x = \xi$$
$$1-\exp(-x/\lambda) = \xi$$
$$x = -\lambda\ln(1-\xi) = -\lambda\ln(\xi')$$

where ξ' is another random number. (Since ξ is distributed uniformly between 0 and 1, so is $(1-\xi)$.)

5.3 Soft photon energy

Before you are able to perform the interaction and calculate the energies of the products, you need to know the energy ϵ of the soft photon that the incident particle (either a gamma-ray or an electron) is interacting with, and the angle θ between the directions of the two particles.

Firstly, the energy of the soft photon. By inspection of Eq. (4.5), the energy of the soft photon is distributed according to

$$p(\epsilon) = \frac{\lambda(E)}{8\beta E^2}\frac{n(\epsilon)}{\epsilon^2}\int_{s_{\min}}^{s_{\max}} \sigma(s)(s-m^2c^4)\ ds$$

where $\lambda(E)$ is the mean free path of the relevant incident particle with energy E, and σ is the total cross-section for the process in question. This distribution has been normalised so that $\int_{\epsilon_{\min}}^{\infty} p(\epsilon)\ d\epsilon = 1$.

However, instead of sampling from this distribution, I instead calculate the *mean* soft photon energy from this distribution, by the integral

$$\begin{aligned}\bar{\epsilon} &= \int_{\epsilon_{\min}}^{\infty} \epsilon\ p(\epsilon)\ d\epsilon. \\ &= \frac{\lambda(E)}{8\beta E^2}\int_{\epsilon_{\min}}^{\infty}\frac{n(\epsilon)}{\epsilon}\int_{s_{\min}}^{s_{\max}}\sigma(s)(s-m^2c^4)\ ds.\end{aligned}$$

The advantage of doing this is that it is much easier and quicker than sampling from the distribution, as $\bar{\epsilon}$ is able to be calculated at the same time as the mean interaction length λ.

In this way, $\bar{\epsilon}$ can be calculated for a given soft photon spectrum and interaction cross section. These are shown for pair production and inverse compton scattering in Fig. 5.1. Note that the range of energies for $\bar{\epsilon}$ in the case of pair production is much greater than that for inverse compton.

For low energies in the inverse compton case, $\bar{\epsilon}$ is constant. This is the so-called Thomson regime, where the compton scattering cross section is given by σ_{T}, the Thomson cross section. Then, the analytic expression for $n(\epsilon)$ in the CMB (Eq. (4.8)) can be used to find the exact value for $\bar{\epsilon}$ (following the method used for the mean free path in Section 4.3.1).The result is that for low energies (below about 1000 GeV), the value of the mean soft photon energy is $\bar{\epsilon} = 6.366\times10^{-13}$ GeV.

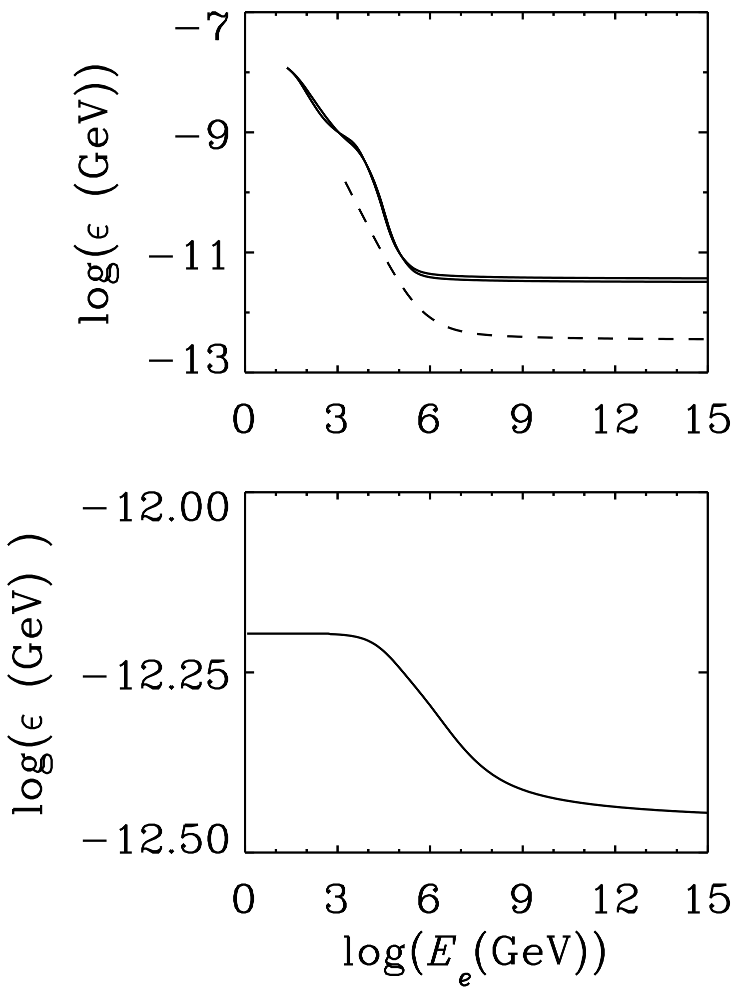

Figure 5.1: **Top:** $\bar{\epsilon}$ for photon-photon pair production. Solid upper and lower curves respectively are for the lower and upper envelopes of the IRB prediction from Macminn and Primack [12]. The dashed curve is for the CMB. **Bottom:** $\bar{\epsilon}$ for inverse compton scattering in the CMB. Note the different scales on the two plots.

5.4 Interaction angle

Once the energies of the two interacting particles are known, a third parameter is needed - the angle θ between their respective directions. Given that the energies of the incident particle and the soft photon are E and $\bar{\epsilon}$ respectively, θ is defined in terms of s, the total CM frame energy squared (defined in Eq. (4.6)), by

$$\theta = \cos^{-1}\left[1 - \frac{(s - m^2c^4)}{2E\bar{\epsilon}}\right] \tag{5.2}$$

where m is the mass of the incident particle.

Thus, θ can be sampled by first sampling a value of s, and then calculating θ by Eq (5.2). The advantage of this is that the distribution of s is already known from the calculation of the mean interaction length. Properly normalised, this distribution is

$$p(s) = \frac{(s - m^2c^4)\sigma(s)}{\int_{s_{\min}}^{s_{\max}} (s - m^2c^4)\sigma(s)\ ds} \tag{5.3}$$

so that $\int_{s_{\min}}^{s_{\max}} p(s)\ ds = 1$.

For pair production, where $m = 0$, this becomes

$$p(s) = \frac{s\sigma(s)}{\int_{2m_e^2c^4}^{4E\bar{\epsilon}} s\sigma(s)\ ds} \tag{5.4}$$

To sample s, the transformation method is used, as detailed in Section 5.2, in which s is sampled according to

$$\int_{s_{\min}}^{s} p(s')\ ds' = \int_0^{\xi} w(\xi')\ d\xi' = \xi.$$

So, for pair production,

$$\int_{2m_e^2c^4}^{s} s'\sigma(s')\ ds' = \xi \int_{2m_e^2c^4}^{4E\bar{\epsilon}} s'\sigma(s')\ ds'.$$

Now, the integral on the left (which is a function of s) can not be inverted analytically to give an expression for s, so it has to be done numerically.

The first step in doing this is to evaluate the integral

$$\int_{2m_e^2c^4}^{s_{\max}} s'\sigma(s')\ ds'$$

for an array of $s_{\max}$ values, up to $s_{\max} = 4E\bar{\epsilon}$, storing the integrals in an array. A value of the integral is then sampled, by sampling ξ, and then a value of s is obtained by interpolating in the $s_{\max}$ array.

The interpolation can be done quite accurately with a relatively small number of array points if the arrays used are $\log(\int s\sigma(s)\ ds)$ and $\log(s_{\max})$, since the integral forms a power law of s.

For inverse compton scattering, a similar process is used. However, since in this case $s = m_e^2c^4 + 2E\epsilon(1 - \beta\cos\theta)$, a change of variable can be used:

$$s \rightarrow x = s - m_e^2c^4 = 2E\epsilon(1 - \beta\cos\theta)$$

so that a value of x is sampled such that

$$\int_{2E\epsilon(1-\beta)}^{x} x'\sigma(x' + m_e^2c^4)\ dx' = \xi \int_{2E\epsilon(1-\beta)}^{2E\epsilon(1+\beta)} x'\sigma(x' + m_e^2c^4)\ dx'.$$

To see why this change of variable is useful, consider how small values of x are represented on the computer. If s was being represented for sufficiently small values of x, it would take the value of $m_e^2c^4$, since decimal numbers can only have a limited number of decimal places. However, if such numbers are represented by x, an exponential representation can be utilised, with the result that far smaller values of x can be expressed. This is useful, since in practice $(1 - \beta)$ is very small for the electrons under consideration, and so $s_{\min}$ will be small.

5.5 Scattering Angle

Once the initial parameters E, ϵ, and θ have been determined, calculation of the interaction, and in particular the energies of the final particles, can proceed. As seen in Chapter 4, to calculate the final energy of a particle, one needs to know the angle through which it has been scattered, that is, the angle between its direction before the interaction, and its direction after the interaction.

5.5.1 Pair production

The scattering angle α is used in the differential cross section $d\sigma_{\gamma\gamma}/d\cos\alpha$ (Eq. (4.1)) (taken in the CM frame) and this gives adistribution for $\cos\alpha$ of

$$p(\cos\alpha) = \frac{1}{\sigma_{\gamma\gamma}}\frac{d\sigma_{\gamma\gamma}}{d\cos\alpha} \tag{5.5}$$

$$= \frac{1}{\sigma_{\gamma\gamma}}\frac{\pi r_0^2}{2}\beta\left(\frac{m_e c^2}{E_\gamma}\right)\frac{1-\beta^4\cos^4\alpha+2(m_e c^2/E_\gamma)^2\beta^2\sin^2\alpha}{(1-\beta^2\cos^2\alpha)^2} \tag{5.6}$$

where $\beta = \sqrt{1-(4m_e^2c^4)/s}$, and E_γ is the photon energy in the CM frame. Again, $p(\cos\alpha)$ is normalised so that $\int_0^1 p(\cos\alpha)\; d\cos\alpha = 1$. Note that this integral is from $\cos\alpha = 0$ to $\cos\alpha = 1$, since there are two identical particles involved. In determining the total cross section, one only integrates over those angles that correspond to physically different events, so if there are two identical (and hence indistinguishable) particles, the integration is only made over one hemisphere, hence the integral is made from $\cos\alpha = 0$ to $\cos\alpha = 1$ instead of -1 to 1. (Note that electrons and positrons can be considered indistinguishable particles for this problem, as they are exactly the same except for their charge, and the cross section, and hence the distribution, is independent of charge.)

This distribution can not be sampled from easily, using any simple rule, so I instead calculate $\cos\alpha_{\mathrm{m}}$, the *median* value of $\cos\alpha$. This is defined by the relation

$$\int_0^{\cos\alpha_{\mathrm{m}}}\frac{d\sigma_{\gamma\gamma}}{d\cos\alpha}\,d\cos\alpha = \frac{1}{2}\int_0^1\frac{d\sigma_{\gamma\gamma}}{d\cos\alpha}\,d\cos\alpha = \frac{1}{2}\sigma_{\gamma\gamma}, \tag{5.7}$$

i.e. $\cos\alpha_{\mathrm{m}}$ is the value of $\cos\alpha$ that divides the area under $d\sigma_{\gamma\gamma}/d\cos\alpha$ in half.

This value is found by a simple search method. The value of $\cos\alpha$ is slowly increased from some initial value, and $d\sigma_{\gamma\gamma}/d\cos\alpha$ is evaluated at that point and compared with $\frac{1}{2}\sigma_{\gamma\gamma}$. If it is smaller, increase $\cos\alpha$ and continue; whereas if it is larger, move back a step, decrease the step size, and continue until the step size is less than some fixed value.

For values of $\cos\alpha$ close to 1, $d\sigma_{\gamma\gamma}/d\cos\alpha$ increases and becomes very sharply peaked. This means that $\cos\alpha_{\mathrm{m}}$ is very close to 1 (i.e. α_{m} is close to 0). For higher energies, this peak becomes sharper, and $\cos\alpha_{\mathrm{m}}$ becomes closer to 1. To calculate $\cos\alpha_{\mathrm{m}}$ accurately, an appproximation needs to be made for these high energies, as the difference between $\cos\alpha_{\mathrm{m}}$ and 1 becomes similar in size to the step size.

Since at high energies, $E_\gamma \gg m_e c^2$ (i.e. photon energy $\gg$ electron rest mass energy), we make the approximation of neglecting the $2(m_e c^2/E_\gamma)^2\beta^2\sin^2\alpha$ term in $d\sigma_{\gamma\gamma}/d\cos\alpha$, so that

$$\frac{d\sigma_{\gamma\gamma}}{d\cos\alpha} = \frac{\pi r_0^2}{2}\beta\left(\frac{m_e c^2}{E_\gamma}\right)\frac{1-\beta^4\cos^4\alpha}{(1-\beta^2\cos^2\alpha)^2}.$$

Now, let $x = \cos\alpha$ (and $x_{\mathrm{m}} = \cos\alpha_{\mathrm{m}}$), so that

$$\begin{aligned}\frac{d\sigma_{\gamma\gamma}}{dx} &= \frac{\pi r_0^2}{2}\beta\left(\frac{m_e c^2}{E_\gamma}\right)\frac{1-\beta^4x^4}{(1-\beta^2x^2)^2}\\ &= \frac{\pi r_0^2}{2}\beta\left(\frac{m_e c^2}{E_\gamma}\right)\frac{(1-\beta^2x^2)(1+\beta^2x^2)}{(1-\beta^2x^2)^2}\\ &= \frac{\pi r_0^2}{2}\beta\left(\frac{m_e c^2}{E_\gamma}\right)\frac{1+\beta^2x^2}{1-\beta^2x^2}\end{aligned}$$

Integrate this:

$$\begin{aligned}\int_0^{x_\mathrm{m}} \frac{d\sigma_{\gamma\gamma}}{dx}\,dx &= \frac{\pi r_0^2}{2}\beta\left(\frac{m_e c^2}{E_\gamma}\right)\int_0^{x_\mathrm{m}} \frac{1+\beta^2 x^2}{1-\beta^2 x^2}\,dx \\ &= \frac{\pi r_0^2}{2}\left(\frac{m_e c^2}{E_\gamma}\right)\left[\log(1-\beta^2 x_\mathrm{m}^2) - \beta x_\mathrm{m}\right]\end{aligned}$$

So, the criterion for $\cos\alpha_\mathrm{m}$, Eq. (5.7), reads

$$\log(1-\beta^2 x_\mathrm{m}^2) - \beta x_\mathrm{m} = \frac{1}{2}\log(1-\beta^2) - \frac{1}{2}\beta$$

$$\log\left(\frac{1-\beta^2 x_\mathrm{m}^2}{\sqrt{1-\beta^2}}\right) = \beta(x_\mathrm{m} - \frac{1}{2}). \tag{5.8}$$

So, for high energies, where $E_\gamma \gg m_e c^2$, $\cos\alpha_\mathrm{m}$ can be found by solving this transcendental equation. This is generally faster and more accurate than solving by the regular method indicated above. A simple root finding algorithm is used, to find the root of the function

$$f(x_\mathrm{m}) = \log\left(\frac{1-\beta^2 x_\mathrm{m}^2}{\sqrt{1-\beta^2}}\right) - \beta(x_\mathrm{m} - \frac{1}{2}),$$

that is, find x_m such that $f(x_\mathrm{m}) = 0$.

Fig. 5.2 shows α_m plotted as a function of energy. It shows the approximation that I made (i.e. Eq. (5.8)), comparing it with the exact formula (i.e. using Eq. (5.7)), and it demonstrates how the approximation is used at high energies.

5.5.2 Inverse compton scattering

A similar approach is used for inverse compton scattering. The distribution of $\cos\alpha$ is given by the differential cross section $d\sigma_{\gamma e}/d\cos\alpha$:

$$\begin{aligned}p(\cos\alpha) &= \frac{1}{\sigma_{\gamma e}}\frac{d\sigma_{\gamma e}}{d\cos\alpha} &(5.9)\\ &= \frac{1}{\sigma_{\gamma e}}\pi r_0^2\left(\frac{\epsilon_1}{\epsilon}\right)^2\left(\frac{\epsilon_1}{\epsilon} + \frac{\epsilon}{\epsilon_1} - (1-\cos^2\alpha)\right) &(5.10)\end{aligned}$$

where

$$\frac{\epsilon_1}{\epsilon} = \frac{1}{1+\frac{\epsilon}{m_e c^2}(1-\cos\alpha)}.$$

This is normalised so that $\int_{-1}^{1} p(\cos\alpha)\ d\cos\alpha = 1$. Note that this integral is from -1 to 1, since the two particles under consideration are distinguishable, that is, they are an electron and a photon, as opposed to two electrons or two photons in the pair production case.

Again, the median value of $\cos\alpha$ is found, using the following relation

$$\int_{-1}^{\cos\alpha_\mathrm{m}} \frac{d\sigma_{\gamma e}}{d\cos\alpha}\,d\cos\alpha = \frac{1}{2}\int_{-1}^{1}\frac{d\sigma_{\gamma e}}{d\cos\alpha}\,d\cos\alpha \tag{5.11}$$

The method for finding $\cos\alpha$ is essentially the same as that for pair production - a simple step search. However, again the search breaks down at high energies, where the differential cross section becomes very sharply peaked at $\cos\alpha = 1$, so an approximation

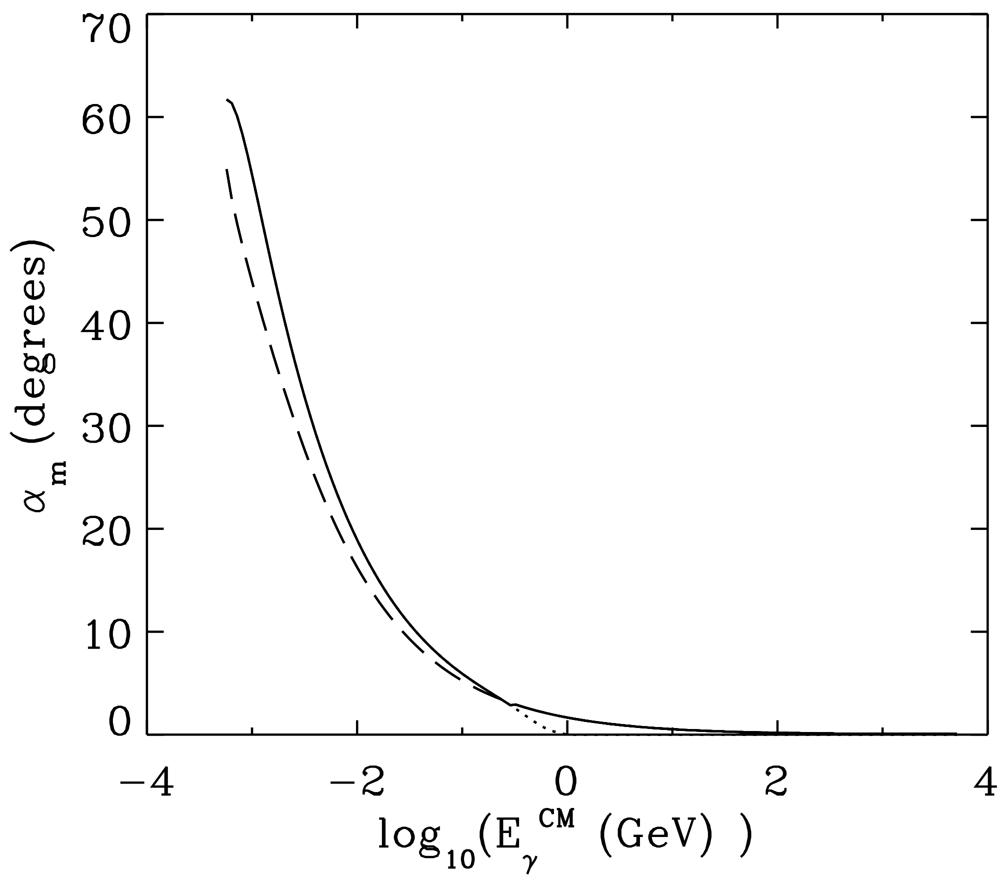

Figure 5.2: Median scattering angle for pair production against photon energy. The solid line is the curve used in the evaluation of $\alpha_{\rm m}$. The dotted line shows what happens at high energies if $\cos\alpha_{\rm m}$ is calculated using Eq. (5.7). The dashed line shows the continuation of the approximation (Eq. (5.8)) into low energies, where it is not applicable. The plot cuts off at $E_\gamma = m_e c^2$, the minimum photon energy in the CM frame.

needs to be made. For $\epsilon \gg m_e c^2$, the differential cross section becomes (letting $x = \cos\alpha$ for brevity)

$$\frac{d\sigma_{\gamma e}}{dx} \approx \frac{\pi r_0^2}{1 + \frac{\epsilon}{m_e c^2}(1-x)}.$$

Integrate this:

$$\begin{aligned}
\int_{-1}^{x_{\rm m}} \frac{d\sigma_{\gamma e}}{dx}\, dx &= \pi r_0^2 \int_{-1}^{x_{\rm m}} \frac{dx}{1 + \frac{\epsilon}{m_e c^2}(1-x)} \\
&= \pi r_0^2 \left[\frac{-m_e c^2}{\epsilon} \log\left(1 + \frac{\epsilon}{m_e c^2}(1-x)\right)\right]_{-1}^{x_{\rm m}} \\
&= \pi r_0^2 \frac{m_e c^2}{\epsilon}\left[\log\left(1 + 2\frac{\epsilon}{m_e c^2}\right) - \log\left(1 + \frac{\epsilon}{m_e c^2}(1-x)\right)\right]
\end{aligned}$$

So, Eq. (5.11) reads

$$\log\left(1 + 2\frac{\epsilon}{m_e c^2}\right) - \log\left(1 + \frac{\epsilon}{m_e c^2}(1-x_{\rm m})\right) = \frac{1}{2}\log\left(1 + 2\frac{\epsilon}{m_e c^2}\right) - \log\left(1 + \frac{\epsilon}{m_e c^2}(1-1)\right)$$

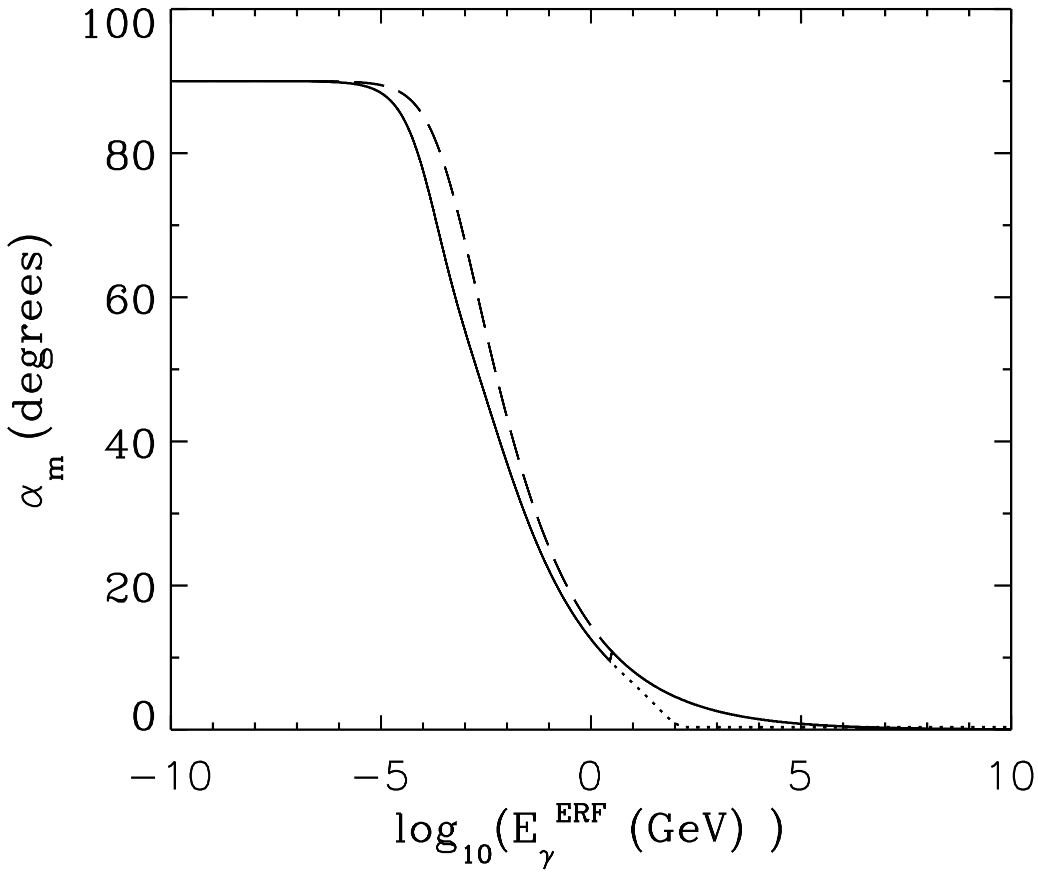

Figure 5.3: Median scattering angle for inverse compton scattering as a functionof photon energy in the ERF. The solid line is the curve used to evaluate $\alpha_{\rm m}$. The dotted line shows what happens at high energies if $\cos\alpha_{\rm m}$ is calculated using Eq. (5.11). The dashed line shows the continuation of the approximation (Eq. (5.12)) into low energies, where it is not applicable.

$$\begin{aligned}\log\left(1+\frac{\epsilon}{m_ec^2}(1-x_{\rm m})\right) &= \frac{1}{2}\log\left(1+2\frac{\epsilon}{m_ec^2}\right)\\ 1+\frac{\epsilon}{m_ec^2}(1-x_{\rm m}) &= \sqrt{1+2\frac{\epsilon}{m_ec^2}}\\ x_{\rm m} &= 1+\frac{m_ec^2}{\epsilon}-\frac{m_ec^2}{\epsilon}\sqrt{1+2\frac{\epsilon}{m_ec^2}} \qquad (5.12)\end{aligned}$$

Thus, at high energies, there is an analytic expression for $\alpha_{\rm m}$, which speeds up the process enormously. Fig. 5.3 shows how this approximation is needed at high energies, and how it is not valid at low energies. As you can see, the agreement between the exact result and the approximation is never exact, although I have chosen the valuefor the change-over to minimise the difference between the two. The values that I used are indicated by the solid line.

Note that below about 10^{-6} GeV, $\alpha_{\rm m}$ is constant at 90°. This is because, for low energies the photon is in the Thomson regime, where $\epsilon_1 \approx \epsilon$, so the differential cross section becomes

$$\frac{d\sigma_{\gamma e}}{dx} = \pi r_0^2(1+x^2).$$

Thus,

$$\int_{-1}^{x_{\mathrm{m}}} \frac{d\sigma_{\gamma e}}{dx}\, dx = \pi r_0^2 \left(\frac{4x_{\mathrm{m}}}{3} + \frac{4}{3}\right)$$

and

$$\int_{-1}^{1} \frac{d\sigma_{\gamma e}}{dx} = \frac{8\pi r_0^2}{3} = \sigma_{\mathrm{T}}$$

Then Eq. (5.11) simply gives $x_{\mathrm{m}} = 0$, or $\alpha_{\mathrm{m}} = 90°$.

5.6 Azimuthal angle

Recalling the analysis of the interactions from Section 4.4, a set of coordinates can be defined such that, in the frame of interest (either the CM frame for pair production or the electron rest frame (ERF) for inverse compton scattering), the photon before the interaction moves along a given axis. Then, the resulting particle (photon or electron) has its momentum vector lying on a cone, centred on the axis, of half angle α_{m}, calculated above.

To find where on this cone the vector lies, we sample uniformly an angle between 0 and 2π, and measure this from some axis perpendicular to the particle's initial direction. Thus, the azimuthal angle δ is defined by

$$\delta = 2\pi\xi$$

where ξ is a random number, discussed in Section 5.2.

Thus, I have sampled two parameters from their respective distributions, namely θ and δ (ignoring the distance for the moment), and found either the mean or the median values of the other two, ϵ and α. The next step is to combine these routines together to model a cascade of electrons and photons in a background radiation field.

Chapter 6

Electromagnetic cascades

Electron photon cascades in the microwave and infrared backgrounds, and their effects on the gamma ray spectra of distant sources have been considered in recent years by a number of authors. Protheroe [31] used monte carlo methods to model cascades in the CMB, from sources such as Cygnus X-3, the Large Magellanic Cloud and Centaurus A. This was done by using matrices to describe propagation of the particles over a small distance, and then repeating the calculations to describe larger distances. This procedure was modified by Protheroe and Stanev [33], who considered cascading in the IRB for distances corresponding to several AGN (Mrk 421, 3C 273, 3C 279, and NGC 4151 (an AGN not detected by EGRET)). A more recent result comes from Biller [34]. This considers the effect of the IRB on the gamma ray spectra of AGN, using a different approach to the computing by parametrising the interaction length and using pre-computed libraries to find the energy-momenta of the secondary particles.

6.1 Program structure

In the previous two chapters, methods for calculating the results of photon-photon pair production and inverse compton scattering have been discussed. These have been considered as individual interactions, with an incident particle interacting with a soft photon to produce two final particles.

However, it is obvious that the electrons produced in the pair production interaction may undergo interact themselves, producing a gamma ray which then pair produces, giving more electrons, and so on, producing an electromagnetic cascade. The extent to which the electrons produce gamma rays by inverse compton scattering is limited by the presence of magnetic fields, in which the electrons will both spiral (thereby changing their direction so that they are not travelling in the same direction as the initial particle), and lose energy by synchrotron emission. In this model, it is assumed that the extragalactic magnetic field is sufficiently low that these effects can be neglected. Thus, the electrons lose energy by inverse compton scattering alone, and travel in straight lines.

The program shown schematically in Fig. 6.1 models a cascade consisting of photon-photon pair production and inverse compton scattering, for an intial injection of a single gamma ray of given energy. This was then run several hundred times (typically 250) to obtain good statistics for the random components of the program (sampling the interaction angle θ and the azimuthal angle δ). This simulates 250 photons of the same energy being injected in the photon field.

For the variables that were not sampled from a distribution (such as λ, $\bar{\epsilon}$, and α), I

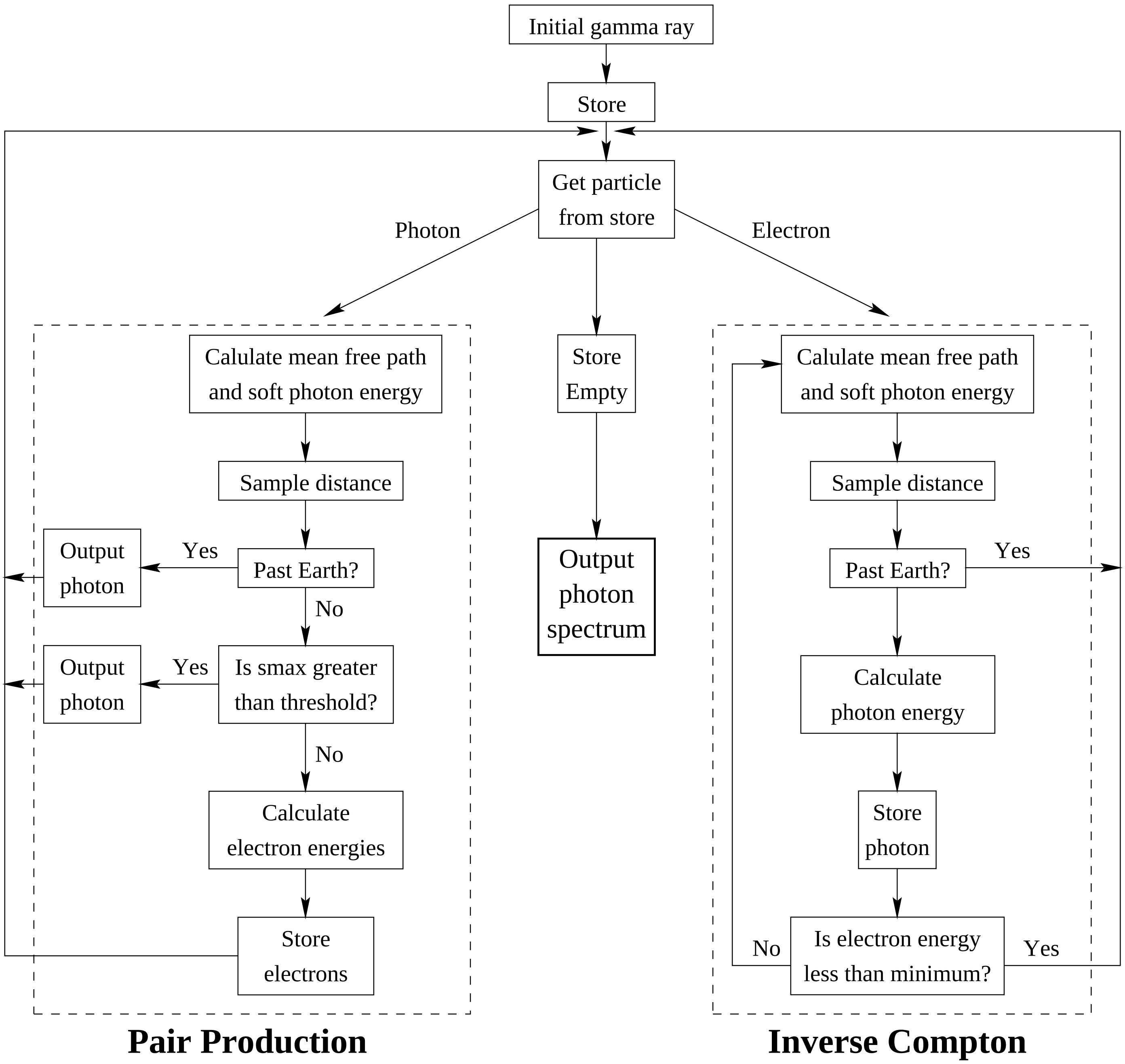

Figure 6.1: Flow diagram for the cascade program with a single gamma ray input.

used arrays to store values of these variable for a range of energies and then interpolate in these arrays when a value of the variable is needed. This removes the need for unnecessary calculations (since the arrays can be calculated beforehand, and read in at the start of the program) and so speeds up the program.

The program only deals with one particle at a time, so when particles have been produced (either in a pair production in the case of electrons or scattered up to gamma ray energies in an inverse compton interaction), their energy, type (i.e. electron or photon) and distance travelled are stored in an array. Each time an interaction is complete, the particle at the top of this array is retrieved.

Since the cascade is taken over some fixed distance, the distance travelled by each particle is stored, and incremented each time the interaction length is sampled. The particles are assumed to travel in the same direction as the initial gamma ray - that is, in a straight line from the source to Earth. This is an approximation, but not one that will affect the results greatly, since the directions of the emitted particles will be highly collimated in the direction of the high energy particle.

When the photons have either travelled past Earth (have travelled a greater distance than that from the source to Earth), or are not energetic enough to undergo pair production (i.e. $s_{\max} < (2m_ec^2)^2$, where s is the total CM frame energy squared), their energy is stored in an array ready for output. (If $s_{\max} < (2m_ec^2)^2$, the photons will not interact again, so they travel straight through to Earth.) When the cascade has finished, that is, there are no more particles in the store, the spectrum of photons at Earth is stored in a file.

The spectrum of electrons at Earth is not under consideration, so if an electron travels further than Earth, it is disregarded, and a new particle is retrieved from the store. Since the electron is not destroyed in the interaction, it is available to scatter again, provided it is above a minimum energy that is imposed on electrons. If that is the case, the electron is used straight away, without being stored.

The electrons have a minimum energy imposed upon them to reduce the amount of particles produced and hence the computing time. Low energy photons have a short mean free path, and so produce a lot of gamma rays (of low energy) in a given distance, all of which need to be considered before the program terminates. If the minimum electron energy is set at the lowest photon energy of interest, then any photons produced by electrons below the minimum will have less energy, and so will not affect the region of interest. This also reduces the computational time, as there will be much less photons produced, meaning less electrons as well.

6.2 Mono-energetic cascades

Mono-energetic cascades are cascades initiated by gamma-rays of a single energy. This is modelled by the basic program structure shown in Fig. 6.1, where a single photon of the required energy is injected, and the program is run a large number of times to simulate the injection of a large number of photons of the same energy (i.e. a large number of cascades).

When a photon reaches Earth, its energy is recorded. If the photon has energy between, say, $(E-\Delta E/2)$ and $(E+\Delta E/2)$, then the number of photons received in the energy bin of width ΔE, centred on energy E, is incremented. These bins cover the full range of energies of interest. The width of the bins is a constant value of $\log E$, that is, $\Delta(\log E) = \text{const}$, so $\Delta E \propto E$. The value of the constant used in the program was 0.1, so that there were ten bins per decade.

When the program is finished, it takes the number of photons received in each bin

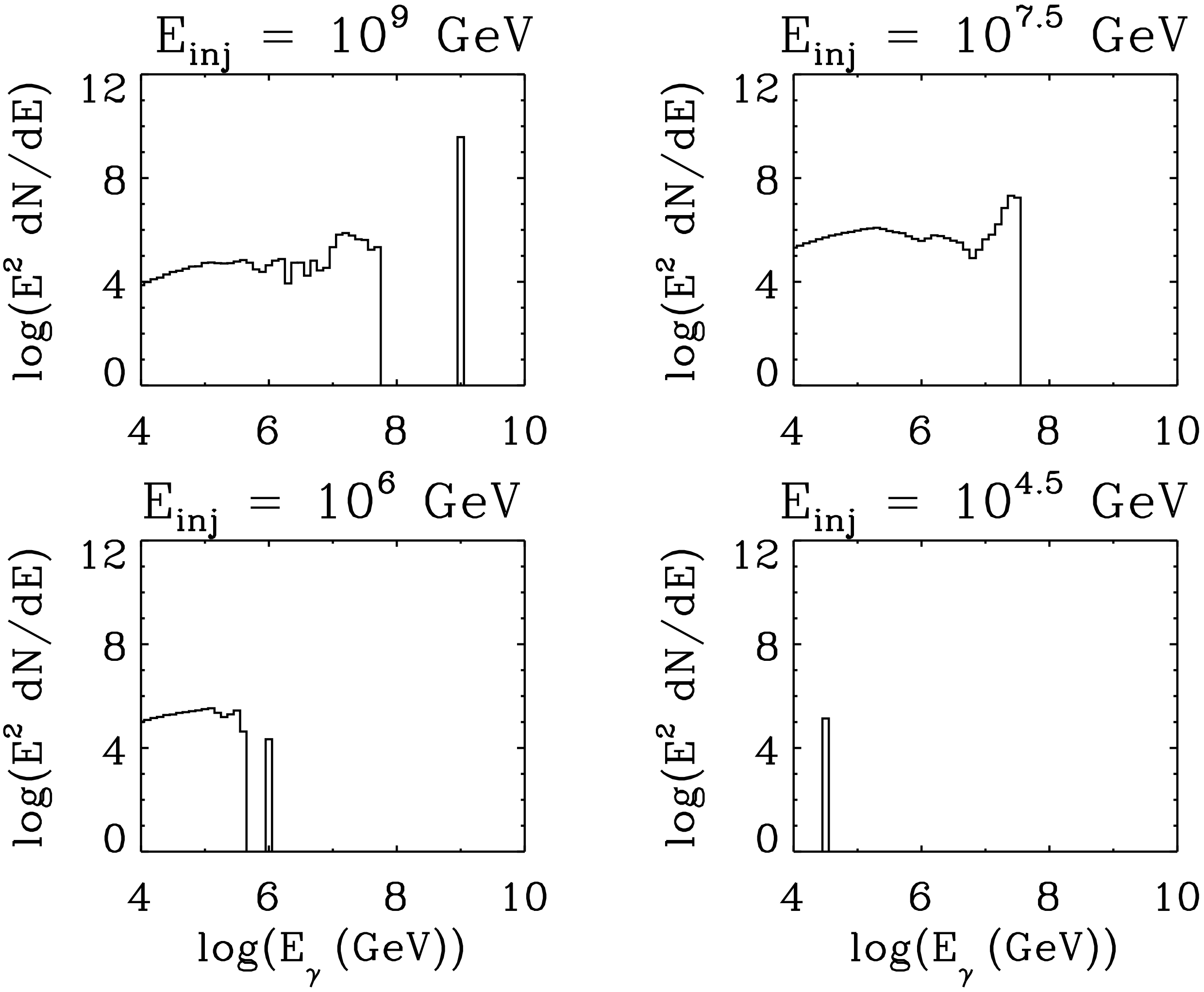

Figure 6.2: Monoenergetic spectra resulting from cascading over a distance of 50 kpc. The initial photon energy, $E_{\rm inj}$, is shown for each plot. The photon spectrum times E^2 (units of GeV) is plotted against photon energy in GeV.

and divides it by the width of the bin and the number of cascades ($N_{\rm casc}$). This gives the differential photon spectrum dN/dE, defined by

$$\frac{dN}{dE} = \frac{\#\ \text{photons}}{N_{\rm casc}\Delta E}.$$

This then gives the spectrum of photons produced by a cascade initiated by a single photon energy. Examples of these are shown in Fig. 6.2, where $\log(E^2\ dN/dE)$ is plotted against $\log(E)$. The reason I multiply the photon spectra by E^2 is that dN/dE is generally decreasing quite steeply, so multiplying it by E^2 smoothes it out and allows deviations from a $dN/dE \propto E^{-2}$ spectrum to be seen more clearly (many gamma ray sources have a spectrum that is approximately E^{-2}).

The spectra in Fig. 6.2 are for different initial gamma ray energies ($E_{\rm inj}$), all propagated over the same distance - in this case, 50 kpc, which is about the distance to the Large Magellanic Cloud - with the photons interacting with the CMB. The difference in the spectra is due to the difference in the mean free paths of the photons through the CMB. The values of the mean free paths are shown in the following table.

$\log(E_{\rm inj}\ (GeV))$	$\lambda_{\gamma\gamma}\ (kpc)$
9.0	343.2
7.5	23.2
6.0	8.2
4.5	5.5×10^{14}

Since the interaction lengths are distributed according to an exponential distribution:

$$p(x) = \frac{1}{\lambda}\exp(-x/\lambda),$$

the number of photons remaining after travelling a distance x is

$$N = N_{\rm casc}\exp(-x/\lambda),$$

where $N_{\rm casc}$ is the number of photons initially. Thus, the photon spectrum for the energy bin containing the initial photon energy is given by

$$\frac{dN}{dE} = \frac{\exp(-x/\lambda)}{\Delta E}.$$

For example, for photons of energy 10^9 GeV and $x = 50$ kpc, this becomes

$$\begin{aligned} \frac{dN}{dE} &= \frac{\exp(-50/343.2)}{\Delta E} \\ &= \frac{0.864}{(10^{9.05} - 10^{8.95})} \\ &= 3.746 \times 10^{-9} \end{aligned}$$

and so the value of $\log(E^2\ dN/dE)$ is $\log(3.746 \times 10^9) = 9.57$. This is approximately the value of the peak at $E = 10^9$GeV on the plot in Fig. 6.2, indicating that the correct amount of absorption is occuring.

The photons present at energies from about $10^{7.5}$ GeV down are the result of the cascading process. The electrons, created by those initial photons that did interact, scatter microwave photons up to gamma ray energies. These energies will be less than the electron energies, which in turn are less than the energies of the injected photons. As the cascade proceeds, the energies of the particles decrease slowly, which is why there are no photons with energies between 10^8 and 10^9 GeV.

At around 10^5 GeV, the mean free path increases rapidly, so any photons produced at these energies are most likely to travel stright through without interacting. Thus, you tend to get a lot of photons around these energies. This is particularly obvious for longer distances, when the photons have more time to lose their energy through pair production and move down to the low energy part of the spectrum.

Since the mean free path for $10^{4.5}$ GeV photons is so large, none of them interact, so the photon spectrum for the energy bin containing $10^{4.5}$ GeV should be given by

$$\begin{aligned} \frac{dN}{dE} &= \frac{N_{\rm casc}}{N_{\rm casc}\Delta E} \\ &= \frac{1}{\Delta E} \end{aligned}$$

which gives, for $E_{\rm inj} = 10^{4.5}$, a value of $\log(E^2\ dN/dE) = 5.14$, which is approximately the value of the peak on the plot in Fig. 6.2.

6.3 Propagation of a power law spectrum

In reality, however, you do not have mono-energetic cascades occuring. Instead, emission from typical astronomical sources takes the form of a power law, $dN/dE \propto E^{-\alpha}$, where α is the spectral index. Typically, the value of α is between 1.5 and 3, and mostly close to 2. This is particularly true for the AGN discovered by EGRET (von Montigny et al. [2]). I will be assuming for my work a spectral index of $\alpha = 2$, since this is the spectral index of Mrk 421 (from [2]).

To model the injection of a power law spectrum, one simply performs mono- energetic cascades for the range of energies of interest, spacing the injection energies with the same spacing as the energy bins. Once you have each of the mono-energetic spectra, you combine them in a way that weights each spectra according to the relative weighting of the initial energy in the initial power law.

Assuming an E^{-2} power law, the injected photon spectrum is set to be

$$\frac{dN^{\mathrm{inj}}}{dE} = E^{-2}.$$

Then, the number of injected photons in the energy bin centered on energy E_i of width ΔE is given by

$$\begin{aligned} N_i^{\mathrm{inj}} &= \int_{E_i-\Delta E/2}^{E_i+\Delta E/2} E^{-2} dE \\ &= \frac{1}{E_i - \Delta E/2} - \frac{1}{E_i + \Delta E/2} \\ &= \frac{\Delta E}{(E_i - \Delta E/2)(E_i + \Delta E/2)}. \end{aligned}$$

Then,

$$\begin{aligned} \frac{N_i^{\mathrm{inj}}}{\Delta E} &= \frac{1}{(E_i - \Delta E/2)(E_i + \Delta E/2)} \\ &\simeq \frac{1}{E_i^2} \end{aligned}$$

(provided ΔE is small), as expected for an E^{-2} power law.

Now, let dN_i/dE_j denote the mono-energetic photon spectrum for the energy bin centered on E_j, due to the mono-energetic injection of photons of energy E_i. Then, the output photon spectrum in the j^{th} energy bin is given by

$$\frac{dN}{dE_j} = \sum_{i \geq j} N_i^{\mathrm{inj}} \frac{dN_i}{dE_j} \tag{6.1}$$

The sum is made over all bins greater than or equal to the energy in question, since any photons that are in a given bin at Earth must have either originated in that bin, in which case they did not interact, or they have been produced by a cascade that was originated by a higher energy photon. This is because there is no process that enables any photons produced to have a greater energy than the primary photon.

In this way, the final photon spectrum can be calculated for each energy bin in the region of interest, to obtain a complete photon spectrum resulting from the injection of a power law.

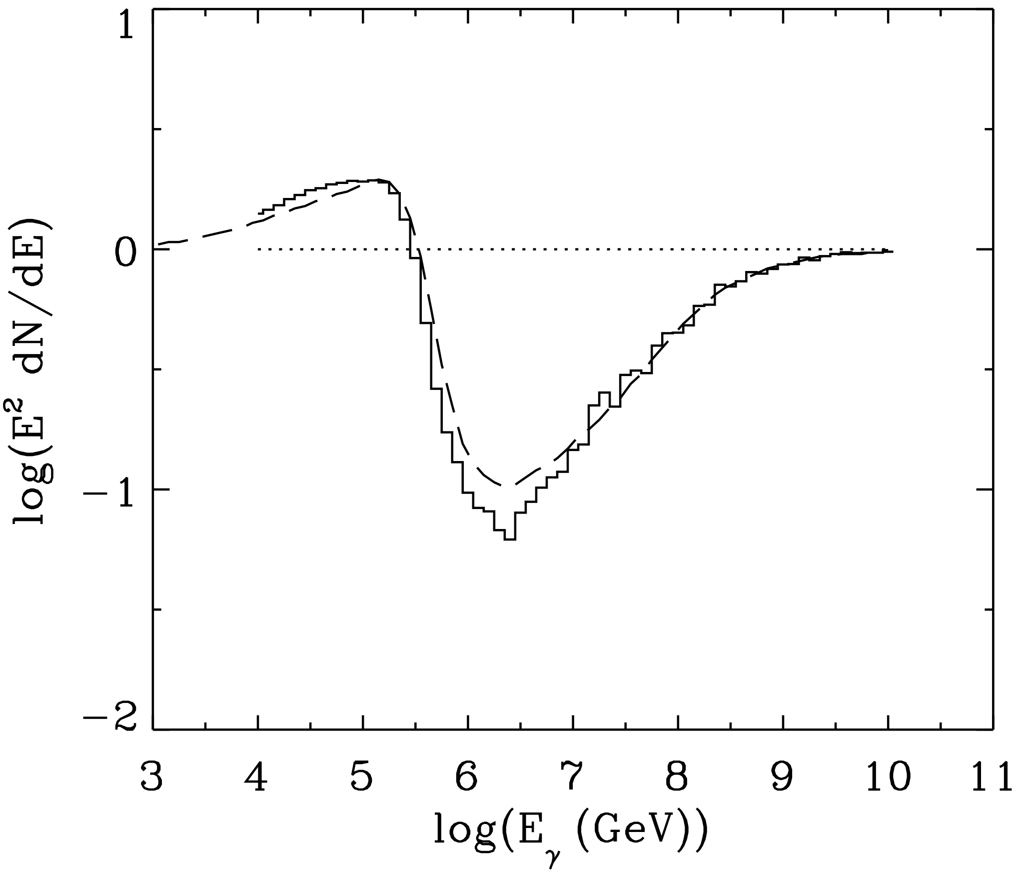

Figure 6.3: An E^{-2} spectrum after cascading over a distance of 50 kpc. The histogram is the resulting spectrum from the program described in the text. The dotted line shows the shape of the initial spectrum, i.e. what the spectrum would look like if no interactions took place. The dashed line is the spectrum from Protheroe [31].

6.4 Results

6.4.1 Cascading in the microwave background

The first case to consider is that shown in Fig. 6.2, cascading through the microwave background over a distance of 50 kpc, which is approximately the distance to the Large Magellanic Cloud. The combined output spectrum is shown in Fig. 6.3, over energies ranging from 10^3 GeV up to 10^{10} GeV.

The histogram in Fig. 6.3 is a histogram of results of mono-energetic injection produced by the program detailed in Section 6.1, and combined to represent the evolution of an E^{-2} power law spectrum by the method explained above.

The qualitative features of the spectrum are as follows. At high energies, the spectrum suffers little absorption, because the mean interaction length is much greater than the distance of propagation. For energies between $10^{5.5}$ GeV to 10^8 GeV, the amount of absorption is considerable, due to the mean interaction length being less than 50 kpc. The amount of absorption, however, is less than would be expected from pair production alone, since the inverse compton scattering by higher energy electrons produces photons in this energy range to replace some of those absorbed in the pair production. At lower energies, the spectrum increases above the value it had upon injection, due to the addition of photons from the inverse compton scattering of higher energy electrons, and because the mean interaction length is much greater than the distance travelled.

The dashed line on Fig. 6.3 is the spectrum after cascading over 50 kpc as calculated by Protheroe [31]. This was calculated using a program that sampled each parameter correctly from its distribution, with no approximations made, unlike my program, where I used the mean soft photon energy and the median scattering angle.

As is evident in Fig. 6.3, my approximate program gives results that almost match the more accurately sampled results from the program by Protheroe. This indicates that the distributions from which I took the mean (in the case of $\bar{\epsilon}$) or the median (in the case of $\alpha_{\rm m}$) would produce values not too different from $\bar{\epsilon}$ and $\alpha_{\rm m}$ had the full sampling been made instead. Thus, my program seems to provide a very good approximation to the more accurately sampled results, at least up to a distance of 50 kpc.

One test to make on this program would be to run it over a larger distance. I had originally intended to run the program over a distance of 6.4 Mpc, which is roughly the distance to Centaurus A, a well known active galaxy, which has been suspected of being a gamma ray emitter, although no definite evidence of this has been found. However, such a program would take a lot longer to run, since the mean interaction lengths are a much smaller proportion of the total distance travelled, meaning that you get a lot more interactions occuring. The problem here is that the electrons, once they get down to low energies, travel on average about 1 kpc, so they undergo a lot of interactions in the given distance before they either reach Earth or drop below the cutoff energy. This large increase in particle numbers requires much more processing time, as well as more storage space, to store the particles before they are interacted.

Thus, time constraints prevented me from completing these calculations. This would be a good direction to extend this work, as there are already previous calculations of spectra from this distance (Protheroe [31]) that used the full sampling routines, and so the effectiveness of the program could be evaluated for longer distances.

6.4.2 Cascading in the infrared background

The second case to consider is that of cascading in the infrared background. For this case, I consider gamma rays emitted from a distance of 100 Mpc, comparable to the distance to Mrk 421, a known TeV gamma ray emitter. The models of the IRB that I considered were the upper and lower envelopes from the predictions of Macminn and Primack [12]

The resulting spectra from these cascades are shown in Fig. 6.4. The solid-line histogram is the spectrum resulting from cascading through the IRB given by the lower envelope of the set of curves given by Macminn and Primack [12]. The dashed-line histogram uses the upper envelope of the set of curves from [12].

Since the upper envelope has the greater intensity, the mean free path through it for photon-photon pair production is shorter, so more absorption is going to take place. This is seen in Fig. 6.4 for energies greater than about 10^3 GeV, where the photon spectrum is less than that for the lower envelope. However, below about $10^{2.5}$ GeV, the upper envelope's spectrum is greater than the lower envelope's. This is because the extra absorption via pair production produces more electrons, which produce more lower energy photons.

An important prediction resulting from these results is that very little emission will be received at energies above about $10^{4.5}$ GeV (or about 30 TeV) from sources at this distance. Thus, at these high energies, any gamma rays detected will be far more likely to

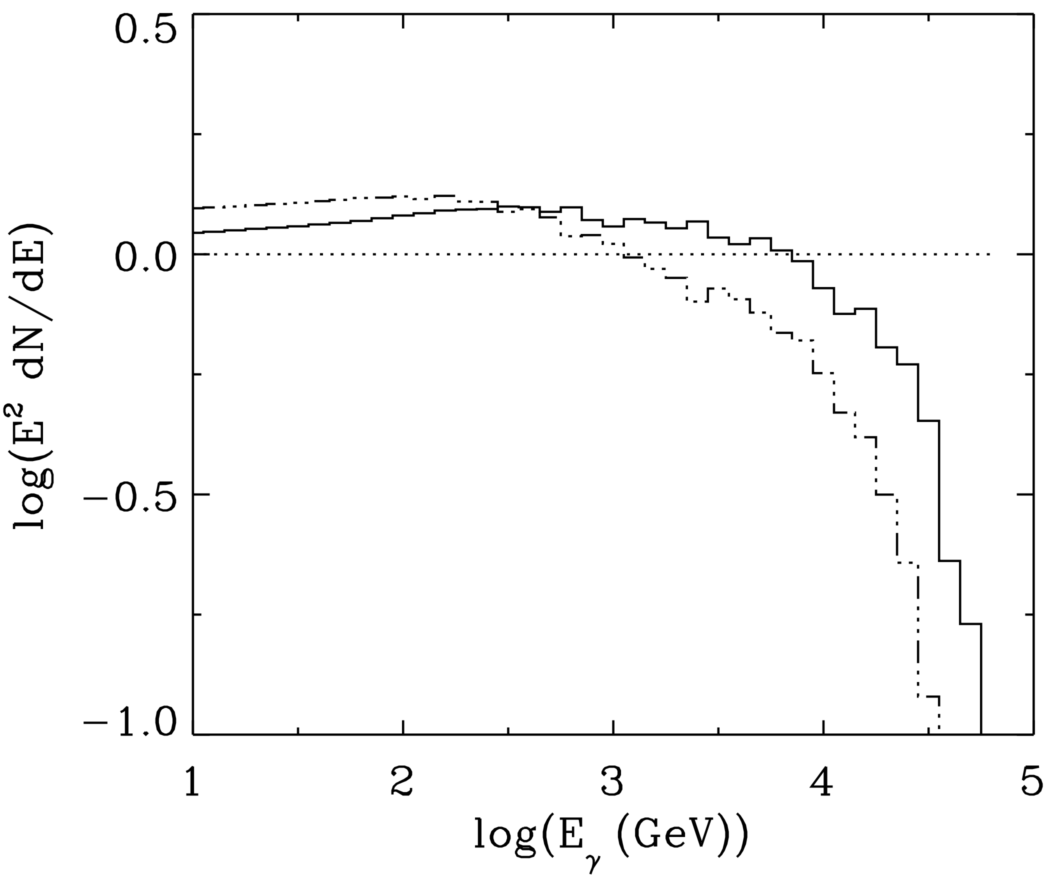

Figure 6.4: An E^{-2} spectrum after cascading over a distance of 100 Mpc. The histogram is the resulting spectrum from the program described in the text. The dotted line shows the shape of the initial spectrum, i.e. what the spectrum would look like if no interactions took place. The solid histogram is from cascading through the lower envelope from Macminn and Primack [12], while the dashed histogram is from cascading through the upper envelop of [12].

have come from more local sources. Also, the further away a source is, the more absorption will take place, and so the cutoff energy will be reduced. This means that, since these spectra correspond to Mrk 421 - the closest of the EGRET AGN - one can just about rule out the possibility of detecting emission at TeV energies from any of the more distant EGRET AGN.

Chapter 7

Conclusions

Motivated by the detection by EGRET of more than 40 AGN at GeV gamma ray energies, and the detection of only one of these at TeV energies, I have investigated the effect of gamma ray-initiated cascades in the infrared and microwave backgrounds on the gamma ray spectra from extragalactic sources.

The infrared background (IRB) has recieved a lot of attention in recent years, both from a theoretical and observational perspective. The predictions of the shape of the IRB spectrum that I have reviewed have been in broad agreement over the range of frequencies of interest, and in general have been consistent with the constraints from observations from COBE. I also made calculations of the background intensity at a wavelength of 60μm.

The spectrum of gamma rays from a distant source is modified in a background photon field by pair production and inverse compton scattering interactions. This produces a cascade of photons and electrons. In modelling such a cascade, it is necessary to take into account the random nature of these interactions by using monte carlo simulations. I constructed a program that made several approximations, including taking the mean energy of the soft photon, and the median scattering angle, instead of sampling from the appropriate distributions. I showed that these approximations had little effect on the resulting gamma ray spectrum.

I have also demonstrated that the IRB causes considerable attenuation of the gamma ray spectrum from Mrk 421 at energies greater than about 30 TeV. This has implications in the area of AGN gamma ray emission, since the amount of absorption will increase for more distant sources, which implies that the cutoff energy for the observed spectra will decrease. Since Mrk 421 is the nearest of all the AGN observed by EGRET at GeV energies, this result indicates that none of the other EGRET AGN will be visible at TeV energies or greater. This is in agreement with the lack of detection of all the EGRET AGN (except Mrk 421) at energies above the EGRET limit of 30 GeV.

Bibliography

[1] Thompson.D.J. et al., *Ap. J. Supp.*, **101**, 259, (1995)

[2] von Montigny.C. et al., *Ap. J.*, **440**, 525, (1995)

[3] Dermer.C.D. and Schlickheiser.R., *Science*, **257**, 1642, (1992)

[4] Punch.M. et al., *Nature*, **358**, 477, (1992)

[5] Petry.D. et al., *Astron. Astrophys.*, in press, preprint astro-ph/9606159, (1996)

[6] Quinn.J. et al., *Ap. J.*, **456**, L83, (1996)

[7] Lin.Y.C. et al., *Ap. J.*, **401**, L61, (1992)

[8] Lloyd-Evans.J. et al., *Nature*, **305**, 784, (1983)

[9] Samorsky.M. and Stamm.W., *Ap. J.*, **268**, L17, (1983)

[10] Aglietta.M. et al., *Astroparticle Phys.*, **3**, 1, (1995)

[11] Allen.W.H. et al., *Ap. J.*, **403**, 239, (1993)

[12] Macminn.D. and Primack.J.R., *Space Science Reviews*, **75**, 413, (1996)

[13] De Zotti.G. et al., preprint astro-ph/9503007, (1995)

[14] Franceschini.A. et al., *Astron. Astrophys Suppl.*, **89**, 285, (1991)

[15] Väisänen.P, *Astron. Astrophys.*, in press (1996)

[16] Hacking.P., Condon.J.J., and Houck.J.R., *Ap. J.*, **316**, L15, (1987)

[17] Protheroe.R.J. and Biermann.P.L., *Astroparticle Phys.*, in press, (1996)

[18] Soifer.B.T. et al., *Ap. J. (Letters)*, **303**, L41, (1986)

[19] Condon.J.J., *Ap. J.*, **287**, 461, (1989)

[20] Saunders.W. et al., *M.N.R.A.S*, **242**, 318, (1990)

[21] Calzetti.D., *A. J.*, in press, preprint astro-ph/9610184, (1996)

[22] Morwood.A.F.M., *Space Science Reviews*, **77**, 303, (1996)

[23] Stecker.F.W. and De Jager.O.C., *Ap. J.* (submitted), preprint astro-ph/9608072, (1996)

[24] Franceschini.A. et al., *Ap. J.*, **427**, 140, (1994)

[25] Puget.J.-L. et al., *Astron. Astrophys.*, **308**, L5, (1995)

[26] Kashlinsky.A. et al., *Ap. J.*, in press, preprint astro-ph/9604182, (1996)

[27] Hauser.M.G., in *Unveiling the cosmic infrared background*, AIP Conf. Proc **348**, pp 11-24, ed. Dwek.E. (1996)

[28] Rybicki.G.B. and Lightman.A.P., *Radiative Processes in Astrophysics*, John Wiley and Sons, 1st Ed., (1979)

[29] Jauch.J.M and Rohrlich.F., *The Theory of Photons and Electrons*, Springer-Verlag, 2nd Ed., (1980)

[30] Fixsen.D.J, et al., *Ap.J.* (submitted), preprint astro-ph/9605054 (1996)

[31] Protheroe.R.J., *M.N.R.A.S.*, **221**, 769, (1986)

[32] Mandl.F. and Shaw.G., *Quantum Field Theory*, John Wiley and Sons, Revised Edition, (1994)

[33] Protheroe.R.J. and Stanev.T., *M.N.R.A.S.*, **264**, 191, (1993)

[34] Biller.S.D., *Astroparticle Phys.*, **3**, 385, (1995)

[35] Kolb.E.W. and Turner.M.S., *The Early Universe*, Addison-Wesley, 1st Ed., (1990)

Appendix A

Cosmological parameters

Two cosmological parameters were used in the calculation of the background intensity at 60μm: the luminosity distance d_{L}, and the rate of change of comoving volume with redshift dV_c/dz. Here I give the formulae for these, taken from Kolb and Turner [35]. The universe is assumed to be a matter-dominated Freidmann-Robertson-Walker cosmology, with a scale factor $a(t)$.

The general expression for the luminosity distance is

$$d_{\mathrm{L}}^2 = a^2(t_0) r_1^2 (1+z)^2$$

where $a(t_0)$ is the scale factor of the universe at the present epoch (i.e. at time t_0). This is the luminosity distance to a source that emitted light at redshift z, with comoving coordinate $r = r_1$. The light is recieved now ($t = t_0$) at coordinte $r = 0$.

The expression for the comoving coordinate r_1 is given by, for a matter dominated universe:

$$r_1 = \frac{2\Omega_0 z + (2\Omega_0 - 4)\left(\sqrt{\Omega_0 z + 1} - 1\right)}{a_0 H_0 \Omega_0^2 (1+z)}$$

where

$$\Omega_0 = \frac{\rho_0}{\rho_c} = \frac{\text{present density of universe}}{\text{critical density}}.$$

Then, the expression for d_{L} becomes

$$d_{\mathrm{L}} = \frac{z q_0 + (q_0 - 1)\left(\sqrt{2 q_0 z + 1} - 1\right)}{q_0^2 H_0}$$

where

$$H_0 = \frac{\dot{a(t_0)}}{a(t_0)}$$

is the Hubble parameter, and

$$q_0 = \frac{-\ddot{a} a}{\dot{a}^2} = \frac{-\ddot{a}}{a H_0^2}$$

is the deceleration parameter.

The unit of comoving volume is given by

$$dV_c = \frac{r^2}{(1 - kr^2)^{1/2}} dr\ d\Omega$$

which means that the rate of change of comoving volume with redshift is, using the full expression for r from above:

$$\begin{aligned}\frac{dV_c}{dz} &= \frac{4\pi\left[zq_0+(q_0-1)\left(\sqrt{2q_0z+1}-1\right)\right]^2}{a_0^3H_0^3(1+z)^3q_0^4\left[1-2q_0+2q_0(1+z)\right]^{1/2}} \\ &= \frac{4\pi d_{\mathrm{L}}^2}{a_0^3H_0(1+z)^3\left[1-2q_0+2q_0(1+z)\right]^{1/2}}\end{aligned}$$

Appendix B

Background intensity program

```
      program intensity
c      background_60micron_lumevol.f
c      calculates the intensity for pure luminosity evolution
      implicit real*8 (a-h,o-z)
c
      data c/299792458.d0/      !value of the speed of light in m/s
      pi=4.d0*datan(1.d0)
      h0=1.d2                   !value of the hubble constant in km/s/Mpc
      q0=0.5d0
      zmin=0.d0
      zmax=9.d0
      smin=1.d-2
      smax=1.d2

      call background(zmin,zmax,q0,h0,smin,smax,bg)
      freq60=c/6.d-5

      write(*,*) dlog10(freq60)
      write(*,*) dlog10(bg)
      end

CCCCCCCCCCCCCCCCCCCCCCCCCCCCCCCCCCCCCCCCCCCCCCCCCCCCCCCCCCCCCC

      function dlum(z,q0,h0)
c      returns luminosity distance for redshift z in units of Mpc

      implicit real*8 (a-h,o-z)
c     convert Hubble const. to units of Mpc
      t0=1.d0/(h0*1.d5/3.d24)
      ct0=3.d10*t0/3.d24

      a=(z*q0 + (q0-1.d0)*(dsqrt(2.d0*q0*z + 1.d0)-1.d0))
      dlum=a*ct0/(q0*q0)

      return
      end
```

```
CCCCCCCCCCCCCCCCCCCCCCCCCCCCCCCCCCCCCCCCCCCCCCCCCCCCCCCCCCCCCC

      function dvcdz(z,q0,h0)
c      returns rate of change of comoving volume with redshift,
c      at redshift z, in units of Mpc^3.

      implicit real*8 (a-h,o-z)

      pi=4.d0*datan(1.d0)

c     convert Hubble const. to units of Mpc
      t0=1.d0/(h0*1.d5/3.d24)
      ct0=3.d10*t0/3.d24

      a=(z*q0 + (q0-1d0)*(dsqrt(2.d0*q0*z + 1.d0)-1.d0))
      dvcdz=4.d0*pi*a*a*ct0**3/(dsqrt(1.d0-2.d0*q0+2.d0*q0*(1+z))
     +        *q0**4*(1+z)**3)

      return
      end

CCCCCCCCCCCCCCCCCCCCCCCCCCCCCCCCCCCCCCCCCCCCCCCCCCCCCCCCCCCCCCCCCC

      function f(z)
c      luminosity evolution function

      implicit real*8 (a-h,o-z)

      z0 = 0.8
      if (z.lt.z0) then
         f = (1+z)**4
      else
         f = (1+z0)**4
      endif

      return
      end

CCCCCCCCCCCCCCCCCCCCCCCCCCCCCCCCCCCCCCCCCCCCCCCCCCCCCCCCCCCCCCCCC

      function g(z)
c      density evolution function

      implicit real*8 (a-h,o-z)

      g = 1.d0
```

```
      return
      end

cccccccccccccccccccccccccccccccccccccccccccccccccccccccccccccccccc

      function rho(alum, z)
c      returns luminosity function for luminosity alum
c     (in W/Hz) and redshift z
c      rho is given in units of Mpc^(-3)*(W/Hz)^(-1)

      implicit real*8 (a-h,o-z)

c      parameter values, given that H0=100 km/s/Mpc, and q0=0.5
c      Using function quoted in Protheroe & Biermann
      Y = 5.93d0
      B = 1.51d0
      W = 0.85d0
      X = 23.96d0

      dummy = dlog10(alum/f(z))

      Q = Y - dsqrt ( B**2 + ((dummy - X)/W)**2)  - 2.5d0 * dummy

      rho = 2.94d28 * 10**Q * g(z)/f(z)
      return
      end

ccccccccccccccccccccccccccccccccccccccccccccccccccccccccccccccccccc

      subroutine sourcecounts(zmin,zmax,q0,h0,snu,sum)
c      returns sourcecounts n(snu) in the variable sum
c      (units = #/Jy/sr) , where snu is the measured flux in Jy,
c      and zmin & zmax are the limits of the integration over redshift.

      implicit real*8 (a-h,o-z)

      pi=4.d0*datan(1.d0)
      n=1000
      dz=(zmax-zmin)/n

      sum=0.0d0
      do i=1,n
         z=zmin + (i-0.5)*dz

         alum=4.d0*pi*snu*dlum(z,q0,h0)**2*9.d18/(1+z)
c         this produces the luminosity in W/Hz

c         alum60 = alum * (1+z)**alpham(alum,z)
```

```
c         this adjusts the luminosity to account for the change in
c         frequency, by using the mean spectral index
c         note that 1+z = freq/freq60

         sigma=0.5d0
         unorm=0.d0
         alphasum=0.d0
         alphamean=alpham(alum,z)
         do dalpha = -2.d0,2.d0,0.2d0
            ualpha = dexp(-dalpha**2/(2.d0*sigma**2))
            alumalpha = alum * (1+z)**(dalpha+alphamean)

            if ((alumalpha.gt.1.d21).and.
     +           (alumalpha.lt.1.d27)) then
               alphasum = alphasum + ualpha * rho(alumalpha,z)
     +              *(1+z)**(dalpha+alphamean)
            endif
            unorm = unorm + ualpha
         enddo
         alphasum = alphasum/unorm

c            now perform the integral
         sum = sum + dz*dvcdz(z,q0,h0)*dlum(z,q0,h0)**2
     +           *9.d44*alphasum/(1+z)
c         sum is now in units of m^2*Hz/W, since 1Mpc = 3.d22 m

      enddo

c      now convert sum into #/Jy/sr, by using the fact that
c      1Mpc^2*Hz/W = 1.d-26 Jy^(-1)sr^(-1)
      sum = sum * 1.d-26

      return
      end


ccccccccccccccccccccccccccccccccccccccccccccccccccccccccccccccccccc

      function alpham(alum,z)

c      calculates the mean spectral index at a given
c      luminosity alum (in W/Hz) and redshift z.

      implicit real*8 (a-h, o-z)

      data alpha25/2.4d0/

      if (z.gt.0.41d0) then
```

```
         alpham = alpha25
      else

         if (alum.lt.1.d22) alpha60 = 2.7d0
         if (alum.gt.(10**25.4)) alpha60 = 1.d0
         if ((alum.lt.(10**25.4)).and.(alum.gt.1.d22))
     +        alpha60 = 2.7d0 - 0.5d0*dlog10(alum/1.d22)

         alpham = alpha25*(dlog10(1.d0+z)/dlog10(1.41d0)) +
     +        alpha60 * (dlog(1.41d0/(1.d0+z))/dlog10(1.41d0))

      endif

      return
      end

cccccccccccccccccccccccccccccccccccccccccccccccccccccccccccccccccccc

      subroutine background(zmin,zmax,q0,h0,smin,smax,bg)

c      Calculates the background intensity (Iv) at 60microns
c      for observed fluxes between smin and smax (in Jy).
c      Returns the intensity in units of W/Hz/m^2/sr. (SI units)

      implicit real*8 (a-h,o-z)

      pi = 4.d0 * datan(1.d0)
      n = 1000
      ds=dlog(smax/smin)/dfloat(n)
      sum=0.d0

      do i=1,n
         s=smin * dexp( (dfloat(i)-0.5d0)*ds)
         call sourcecounts(zmin,zmax,q0,h0,s,c)
         sum = sum + ds*s*s*c
      enddo
c      convert from Jy/sr to W/Hz/m^2/sr
      bg = sum * 4.d0 * pi * 1.d-26
      return
      end
```

Appendix C

Cascade program

This is the program used to calculate the mono-energetic spectrum for the injection energy given (in this case 10^9 GeV).

```
      PROGRAM CASCADE_MBR
c 6/11/96
c Modelling an electromagnetic cascade through the microwave background

      IMPLICIT REAL*8 (A-H,O-Z)
      PARAMETER(NCASC=250)
      DATA EMASS/0.5110034D-3/  ! ELECTRON MASS (GEV)
      DATA BK/8.617E-14/        ! BOLTZMANN CONST (GEV/K)
      DATA PC6/3.086D24/        ! 1 MPC IN CM
      DATA SIGMAT/0.665D-24/    ! THOMSON'S CROSS-SECTION (CM^2)
      T = 2.728D0               ! TEMP OF CMB BLACKBODY
      PI = DACOS(-1.D0)
      STHR_PP = (2.D0*EMASS)**2 ! THRESHOLD FOR PAIR PRODUCTION
      EMIN_EL = 1.D4            ! MINIMUM ELECTRON ENERGY IS 10^5 GEV

      DISTANCE = 50.d-3         ! DISTANCE TO SOURCE IN MPC
      E0 = 10.d0**(9.0)         ! INJECTION GAMMA RAY ENERGY
      DO NUMBER=1,NCASC
         E = E0
         X=0.d0
         ITP=0
         NSTORE=0
         CALL STORE(X,ITP,E,NSTORE,1)

 1       IF(NSTORE.LE.0)GOTO 5
         CALL STORE(X,ITP,E,NSTORE,-1)

 2       IF(ITP.EQ.0)THEN
            CALL PPMFP(E,GGMFP,EBAR)
            DX = SAMPLE_INTLENGTH(ggmfp)
            X=X+DX
            IF (X.LT.DISTANCE) THEN
```

```
         SMAX = 4.D0*E*EBAR
         IF (SMAX.GT.STHR_PP) THEN
            S = SSAMP_PP(SMAX)
            if (s.gt.smax) then
               print *,'s > smax pp',s,smax,S/(2.D0*E*EBAR)
            endif
            THETA = DACOS(1.D0 - S/(2.D0*E*EBAR))
            CALL TRANSFORM_PP(E,EBAR,THETA,E1,E2)
            if (e1.gt.e0) print *,'e1>e0',e1,e,ebar,theta
            if (e2.gt.e0) print *,'e2>e0',e2,e,ebar,theta
            CALL STORE(X,1,E1,NSTORE,1)
            CALL STORE(X,1,E2,NSTORE,1)
         ELSE
            if (e.gt.e0) print *,e,x
            CALL RECORD(E)
         ENDIF
      ELSE
         if (e.gt.e0) print *,e,x
         CALL RECORD(E)
      ENDIF
      GOTO 1
   ELSE
      CALL ELMFP(E,EMFP,EBAR)
      DX = SAMPLE_INTLENGTH(EMFP)
      X=X+DX
      IF (X.LT.DISTANCE) THEN
         ONEMBETA = 0.5D0*(EMASS/E)**2 + 0.125*(EMASS/E)**4
         YMAX = 2.D0*E*EBAR*(2-ONEMBETA)
         YMIN = 2.D0*E*EBAR*ONEMBETA
         Y = XSAMP_IC(YMIN,YMAX)
         if (Y.gt.Ymax) print *,'s>smax ic',Y,Ymax
         if (Y.lt.0) print *,'s<emass**2',Y
         COSTHETA = (1.D0 - Y/(2.D0*E*EBAR))
         if (abs(costheta).gt.1.d0) print *,'costheta',costheta,s
         THETA = DACOS(COSTHETA)
         CALL TRANSFORM_IC(E,EBAR,THETA,EPH)
         if (eph.gt.e0) then
            print *,'eph>e0',eph,theta,ebar
         endif
         E = E + EBAR - EPH
         CALL STORE(X,0,EPH,NSTORE,1)
         IF (E.LT.EMIN_EL) THEN
            GOTO 1
         ENDIF
      ELSE
         GOTO 1
      ENDIF
   ENDIF
```

```
         GOTO 2

 5    ENDDO

      CALL OUTPUT(NCASC)

      STOP
      END

C=================================================================

      SUBROUTINE PPMFP(E,GGMFP,EBAR)
      IMPLICIT REAL*8(A-H,O-Z)
      DIMENSION ENERGY(200),XPP(200),EBARPP(200)
      DATA IFIRST/1/

      IF (IFIRST.EQ.1) THEN
         ifirst = 0
         open (unit=12,file='mbr_pp.dat',status='old')
         read(12,*) nsize
         read(12,*) (energy(i),i=1,nsize)
         read(12,*) (xpp(i),i=1,nsize)
         read(12,*) (ebarpp(i),i=1,nsize)
         close(unit=12)
      endif

      GGMFP = 0.D0
      EBAR = 0.D0

      DELTA_EL = ENERGY(2)-ENERGY(1)
      EL = DLOG10(E)
      IE = (EL-ENERGY(1))/DELTA_EL + 1
      IF (IE.GT.NSIZE) IE=NSIZE-1
      IF (IE.LT.1) IE=1
c interpolate in arrays
      SLOPE1 = (XPP(IE+1)-XPP(IE))/DELTA_EL
      GGMFP = 10.D0**(XPP(IE) + SLOPE1*(EL-ENERGY(IE)))
      SLOPE2 = (EBARPP(IE+1)-EBARPP(IE))/DELTA_EL
      EBAR = 10.D0**(EBARPP(IE) + SLOPE2*(EL-ENERGY(IE)))

      RETURN
      END
C=================================================================

      SUBROUTINE ELMFP(E,EMFP,EBAR)
      IMPLICIT REAL*8(A-H,O-Z)
      DIMENSION ENERGY(200),XIC(200),EBARIC(200)
      DATA IFIRST/1/
```

```
      IF (IFIRST.EQ.1) THEN
         ifirst = 0
         open (unit=12,file='mbr_ic.dat',status='old')
         read(12,*) nsize
         read(12,*) (energy(i),i=1,nsize)
         read(12,*) (xic(i),i=1,nsize)
         read(12,*) (ebaric(i),i=1,nsize)
         close(unit=12)
      endif

      EMFP = 0.D0
      EBAR = 0.D0

      DELTA_EL = ENERGY(2)-ENERGY(1)
      EL = DLOG10(E)
      IE = (EL-ENERGY(1))/DELTA_EL + 1
      IF (IE.GT.NSIZE) IE=NSIZE-1
      IF (IE.LT.1) IE=1
c interpolate in arrays
      SLOPE1 = (XIC(IE+1)-XIC(IE))/DELTA_EL
      EMFP = 10.D0**(XIC(IE) + SLOPE1*(EL-ENERGY(IE)))
      SLOPE2 = (EBARIC(IE+1)-EBARIC(IE))/DELTA_EL
      EBAR = 10.D0**(EBARIC(IE) + SLOPE2*(EL-ENERGY(IE)))

      RETURN
      END

C===================================================================

      SUBROUTINE STORE(X,ITP,E,NSTORE,IDEPOSIT)
c from R.J.Protheroe's electron_photon_cascade.f
      PARAMETER (NMAX=1000)
C     NMAX IS THE MAXIMUM NUMBER OF PARTICLES THAT CAN BE STORED AT
C     ANY ONE TIME IN THE STORE
      IMPLICIT REAL*8(A-H,O-Z)
      DIMENSION XS(NMAX),ITPS(NMAX),ES(NMAX)

      IF(NSTORE.EQ.0.AND.IDEPOSIT.NE.1)
     &     WRITE(6,*)'CANNOT WITHDRAW FROM STORE'
      IF(NSTORE.EQ.NMAX.AND.IDEPOSIT.EQ.1)
     &     WRITE(6,*)'STORE FULL'

      IF(IDEPOSIT.EQ.1)THEN
         NSTORE=NSTORE+1
         XS(NSTORE)=X
         ITPS(NSTORE)=ITP
         ES(NSTORE)=E
```

```
      ELSE
         X=XS(NSTORE)
         ITP=ITPS(NSTORE)
         E=ES(NSTORE)
         NSTORE=NSTORE-1
      ENDIF

      RETURN
      END

*******************************************************************

      SUBROUTINE RECORD(E,ifirst)
      IMPLICIT REAL*8 (A-H,O-Z)

      PARAMETER(NBIN=62)
      DIMENSION NUMBER(NBIN),Esqdnl(NBIN),EPT(NBIN)
      DATA NUMBER/NBIN*0/
      EMINL = 3.95D0
      DELTAE = 0.1D0

      IE = (DLOG10(E)-EMINL)/DELTAE + 1
      IF ((IE.LE.NBIN).AND.(IE.GT.0)) THEN
         NUMBER(IE) = NUMBER(IE) + 1
      ELSE
         PRINT *,'PHOTON OUTSIDE BINNED AREA.', E
      ENDIF
      RETURN

      ENTRY OUTPUT(NCASC)

      DO K=1,NBIN
         EPT(K) = EMINL + (K-0.5d0)*DELTAE
         WIDTH=10.D0**EPT(K)*(10.D0**0.05 - 10.D0**(-0.05))
         EDIST = DFLOAT(NUMBER(K))/(WIDTH*DFLOAT(NCASC))
         IF (EDIST.NE.0.D0) THEN
            ESQDNL(K)=2.D0*EPT(K)+DLOG10(EDIST)
         ELSE
            ESQDNL(K)=-100.D0
         ENDIF
      ENDDO

      OPEN (UNIT=9,FILE='spec-9.0-50k-4.dat',STATUS='unknown')
      write(9,*) NBIN
      WRITE(9,*) (EPT(K),K=1,NBIN)
      WRITE(9,*) (ESQDNL(K),K=1,NBIN)
      CLOSE(UNIT=9)
```

```
      RETURN
      END

*******************************************************************

      FUNCTION SAMPLE_INTLENGTH(AMFP)
      IMPLICIT NONE
c Samples an interaction length from an exponential distribution
c given a mean interaction length of AMFP.
c Both GGMFP and GAMINTLENGTH are in Mpc.
      REAL *8 SAMPLE_INTLENGTH,AMFP
      REAL R,RNUNF
      SAMPLE_INTLENGTH = 0.D0
      R = RNUNF()
      R = RNUNF()
      SAMPLE_INTLENGTH = -AMFP*DLOG(1.d0-R)
      RETURN
      END

C==================================================================

      FUNCTION SSAMP_PP(SMAX)
C
C     CALCULATES INTEGRAL OF S*SIGMA(S) OVER S FROM STHR TO SMAX
C     FOR PAIR PHOTOPRODUCTION.
C     SMAX IN GEV^2
C     UNIT: GEV^4 CM^2
C

      IMPLICIT REAL*8 (A-H,O-Q,S-Z)
      IMPLICIT REAL (R)
      DIMENSION sintl(400),sarrayl(400)

      DATA IFIRST/1/
      DATA EMASS/0.5110034D-3/
      DATA DELTA/0.0001D0/
      data de/0.025d0/

      STHR=(2*EMASS)**2

      IF(IFIRST.EQ.1)THEN
         IFIRST=0
         SUM=0.D0
         VAL=0.D0
         DLOGS=DELTA*2.3025851D0
         DO ISMAX=1,100000
            OLDVAL=VAL
            S=STHR*10.D0**(ISMAX*DELTA)
```

```
            VAL=S*(GGEETOT_CS(S))*S*DLOGS
            SUM=SUM+0.5D0*(OLDVAL+VAL)
            if (mod(ismax,250).eq.0) then
               sarrayl(ismax/250) = dlog10(s)
               sintl(ismax/250) = dlog10(sum)
            endif
         ENDDO
      ENDIF
      SSAMP_PP=0.D0

      GGEE_SIGINT=0.D0
      IF(SMAX.LE.STHR)RETURN
      SMAXL=DLOG10(SMAX/STHR)
      ISMAX=SMAXL/DE+1.D0
      IF(ISMAX.GT.100000) THEN
         WRITE(6,*)'GGEE_SIGINT: (ISMAX.GT.100000).  ',SMAX,ISMAX
      ELSEIF(ISMAX.EQ.1)THEN
         GGEE_SIGINT=(SMAXL/DE+1.D0-ISMAX)*SINTl(ISMAX)
      ELSE
         GGEE_SIGINT=SINTl(ISMAX-1)+(SMAXL/DE+1.D0-ISMAX)*
     &        (SINTl(ISMAX)-Sintl(ISMAX-1))
      ENDIF
      GGEE_SIGINT=10.d0**GGEE_SIGINT

 20   R = RNUNF()
      R = RNUNF()
      VAL = dlog10(GGEE_SIGINT*R)
      SSAMP_PP=0.D0
      k=0
 10   k=k+1
      IF (SINTl(k).LT.VAL) GOTO 10
      if (k.eq.1) k=2
      SLOPE = (SINTl(k) - SINTl(k-1))/DE
      if (slope.eq.0) print *,'GGEE_SINT: SLOPE=0',smax,k
      SSAMPLOG = sarrayl(k-1) + (VAL-SINTl(k-1))/SLOPE
      SSAMP_PP = 10.d0**SSAMPLOG
      IF (SSAMP_PP.LE.STHR)then
c         write(6,*) 'SSAMP_PP: (S.LT.STHR).',SSAMP_PP,STHR
         GOTO 20
      ENDIF
      RETURN
      END

C =================================================================

      FUNCTION GGEETOT_CS(S)

      IMPLICIT REAL*8 (A-H,O-Z)
```

```
      DATA EMASS/0.5110034d-3/

      GGEETOT_CS=0.D0
      IF(S.LE.(2.D0*EMASS)**2)RETURN

c      B=DSQRT(1.D0-(2.D0*EMASS)**2/S)
      x = (2.D0*EMASS)**2/S     !1 - beta^2
      y = 0.5d0*x + 0.125*x**2  !1 - beta

      SIG=-2.D0*(1.d0-y)*(x+1.D0)+(2.d0+x*(2.d0-x))*DLOG((2.d0-y)/y)
      GGEETOT_CS=1.2474D-25*x*SIG

      return
      end

*******************************************************************

      SUBROUTINE TRANSFORM_PP(EPH1,EPH2,THETA,EE1,EE2)
c transforms to electron rest frame, performs pair production
c and transforms back to lab frame.
c EPH1,EPH2 = energies of photons (hard&soft) in lab frame
c THETA = angle between photons' directions in lab frame.
c EE1, EE2 = energies of electrons in lab frame after interaction
      IMPLICIT REAL*8 (A-H,O-Q,S-Z)
      IMPLICIT REAL (R)
      DATA EMASS/0.51100337D-3/ ! ELECTRON MASS (GEV)
      PI = DACOS(-1.D0)
c Calculate energy of each photon in CM frame
      S = 2.D0*EPH1*EPH2*(1-COS(THETA))
      EPRIME = DSQRT(S)/2.D0
      IF (EPRIME.LT.EMASS) THEN
         EE1 = 0.D0
         EE2 = 0.D0
         PRINT *,'EPRIME.LT.EMASS'
         RETURN
      ELSE
c
c Now calculate geometry of boosted frame
c First angle of boost to hard-photon direction
         tanPHI = EPH2*SIN(THETA)/(EPH1+EPH2*COS(THETA))
         phi = datan(tanphi)
         cosphi = cos(phi)
         sinphi = sin(phi)
c Next the beta factor of the boost (velocity)
c         ONEMINUSBB = (EPH1*(1-COS(PHI)) + EPH2*(1-COS(THETA-PHI)))
c     &        /(EPH1 + EPH2)
c         BB = 1.D0 - ONEMINUSBB
```

```
         oneminusbb = (eph1*(1.d0-cosphi)+eph2*(1.d0-cosphi*cos(theta)
     &        -sinphi*sin(theta)))/(eph1+eph2)
c
c Gamma factor of the boost
         GB = 1.D0/DSQRT(2.D0*ONEMINUSBB - ONEMINUSBB**2)
c
c Angle between boost direction and photon direction in CM frame
         ALPHA = DATAN(SIN(PHI)/(GB*(COS(PHI)-1.d0+oneminusBB)))
c Now beta and gamma for the electrons
         GE = EPRIME/EMASS
         onembe = 0.5/ge**2 + 0.125/ge**4
c         BE = DSQRT(1.D0 - 1.D0/GE**2)
c
c now find momentum (in CM frame) and energy (LAB frame) of electrons
c         PC = GE*EMASS*BE       !GeV
         pc = ge*emass*(1.d0-onembe)
         SCAT_ANG = THETAM_PP(EPRIME)
c         scat_ang = 1.d0
         R=RNUNF()
         R=RNUNF()
         AZIMUTH = 2.D0*PI*R

         PXPRIME = COS(SCAT_ANG)*COS(ALPHA) - SIN(SCAT_ANG)*
     &        COS(AZIMUTH)*SIN(ALPHA)

         EE1 = GB*(EPRIME + (1.d0-oneminusBB)*PC*PXPRIME)
         EE2 = GB*(EPRIME - (1.d0-oneminusBB)*PC*PXPRIME)

         RETURN
      ENDIF
      END

********************************************************************

      FUNCTION THETAM_PP(EPH)
      IMPLICIT REAL*8(A-H,O-Z)
      DIMENSION ENERGY(200),THETAM(200)
      DATA IFIRST/1/

      IF (IFIRST.EQ.1) THEN
         ifirst = 0
         open (unit=12,file='thetam_pp.dat',status='old')
         read(12,*) nsize
         read(12,*) (energy(i),i=1,nsize)
         read(12,*) (thetam(i),i=1,nsize)
         close(unit=12)
      endif
      THETAM_PP=0.D0
```

```
      DELTA_EL = ENERGY(2)-ENERGY(1)
      EL = DLOG10(EPH)
      IE = (EL-ENERGY(1))/DELTA_EL + 1
      IF (IE.GT.NSIZE) IE=NSIZE-1
      IF (IE.LT.1) IE=1
c interpolate in array
      SLOPE = (THETAM(IE+1)-THETAM(IE))/DELTA_EL
      THETAM_PP = THETAM(IE) + SLOPE*(EL-ENERGY(IE))

      RETURN
      END

C====================================================================

      FUNCTION XSAMP_IC(XMIN,XMAX)
C
C     CALCULATES INTEGRAL OF S*SIGMA(S) OVER S FROM XMIN TO XMAX
C     FOR INVERSE COMPTON SCATTERING
C     X = S - EMASS**2
C     XMAX,XMIN IN GEV^2
C     UNIT: GEV^4 CM^2
C
      IMPLICIT REAL*8 (A-H,O-Q,S-Z)
      IMPLICIT REAL (R)
      PARAMETER(IMAX=500000)
      DIMENSION xarrayl(500),xintl(500)

      DATA IFIRST/1/
      DATA EMASS/0.5110034D-3/
      DATA DELTA/0.0001D0/
      DATA DE/0.1D0/
      IF(IFIRST.EQ.1)THEN
         IFIRST=0
         XMINLOG = -45.D0
         SUM=0.D0
         VAL=0.D0
         DLOGX=DELTA*2.3025851D0
         DO IXMAX=1,IMAX
            OLDVAL=VAL
            X=10.D0**(XMINLOG+IXMAX*DELTA)
            VAL=X*COMPTON_CS(X)*X*DLOGX
            SUM=SUM+0.5D0*(OLDVAL+VAL)
            if (mod(ixmax,1000).eq.0) then
               xarrayl(ixmax/1000) = dlog10(x)
               xintl(ixmax/1000) = dlog10(sum)
            endif
         ENDDO
```

```
      ENDIF
      XSAMP_IC = 0.D0
      COMPT_SIGINT=0.D0
      IF(XMAX.LE.0.D0)RETURN
      XMAXL= DLOG10(XMAX) - XMINLOG
      IXMAX=XMAXL/DE+1.D0
      IF (IXMAX.EQ.0) PRINT *,'COMPTON_SINT: (IXMAX.EQ.0)',xmaxl,xmax
      IF(IXMAX.GT.IMAX) THEN
         WRITE(6,*)'COMPTON_SINT: (IXMAX.GT.IMAX).  ',SMAX,IXMAX
      ELSEIF(IXMAX.EQ.1)THEN
         UPPER_INT=(XMAXL/DE+1.D0-IXMAX)*XINTL(IXMAX)
      ELSE
         UPPER_INT=XINTL(IXMAX-1)+(XMAXL/DE+1.D0-IXMAX)*
     &        (XINTL(IXMAX)-XINTL(IXMAX-1))
      ENDIF
      IF(XMIN.LE.0.D0)RETURN
      XMINL= DLOG10(XMIN) - XMINLOG
      IXMIN=XMINL/DE+1.D0
      IF(IXMIN.GT.IMAX) THEN
         WRITE(6,*)'COMPTON_SINT: (IXMIN.GT.IMAX).  ',XMIN,IXMIN
      ELSEIF (IXMIN.LT.0) THEN
         WRITE(6,*)'COMPTON_SINT: (IXMIN.LT.0).  ',XMIN,IXMIN
      ELSEIF(IXMIN.EQ.1)THEN
         BOTTOM_INT=(XMINL/DE+1.D0-IXMIN)*XINTL(IXMIN)
      ELSE
         BOTTOM_INT=XINTL(IXMIN-1)+(XMINL/DE+1.D0-IXMIN)*
     &        (XINTL(IXMIN)-XINTL(IXMIN-1))
      ENDIF

      COMPT_SIGINT = 10.D0**UPPER_INT - 10.D0**BOTTOM_INT
      XSAMP_IC = 0.D0
 20   R = RNUNF()
      R = RNUNF()
      VAL = DLOG10(COMPT_SIGINT*R)
      J=0
 10   J=J+1
      IF (XINTL(J).LT.VAL) GOTO 10
      if (j.eq.1) j=2
      SLOPE = (XINTL(J)-XINTL(J-1))/DE
      XSAMPLOG = XARRAYL(J-1) + (VAL-XINTL(J-1))/SLOPE
      XSAMP_IC = 10.D0**XSAMPLOG
      IF (XSAMP_IC.LT.0.D0) THEN
         PRINT *,'COMPTON_SINT: (XSAMPLE.LT.0.D0)',R,XSAMP_IC
         GOTO 20
      ENDIF
      RETURN
      END
```

```
C ==================================================================

      FUNCTION COMPTON_CS(X)
c      cross section for inverse compton scattering, where S is the
c      CM frame energy squared.
c      returns COMPTON_CS in cm^2
      IMPLICIT REAL*8 (A-H,O-Z)
      DATA R/2.818d-13/         !classical radius of electron (cm)
      DATA EMASS/0.51100337d-3/ !mass of electron (GeV)
      PI = DACOS(-1.D0)
c calculate photon energy in electron's rest frame
      W = X/(2.D0*EMASS)
      W = W/EMASS               !need W in units of EMASS
      if (w.le.0.d0) print *, 'compton_cs:w<0',w
      if (w.gt.1.d-3) then
         SIGMA = (1.D0+W)*(2.D0*W*(1.D0+W)/(1.D0+2.D0*W) -
     &        DLOG(1.D0+2.D0*W))/W**3

         SIGMA = SIGMA + DLOG(1.D0+2.D0*W)/(2.D0*W) - (1.D0+3.D0*W)/
     &        (1.D0+2.D0*W)**2
         COMPTON_CS = SIGMA * R**2 * 2.D0 * PI
      else
         compton_cs = 8.d0*pi*r**2/3.d0
      endif
      RETURN
      END

*******************************************************************

      SUBROUTINE TRANSFORM_IC(EE,EPH,THETA,EPHNEW)
c transforms to electron rest frame, performs compton scattering
c interaction and transforms back to lab frame.
c EE = electron energy (GeV), EPH = photon energy (GeV)
c THETA = angle between particles' directions  -  all in lab frame.
c EPHNEW = energy of photon in lab frame after interaction
      IMPLICIT REAL*8 (A-H,O-Q,S-Z)
      IMPLICIT REAL (R)
      DATA EMASS/0.51100337D-3/ ! ELECTRON MASS (GEV)
      PI = DACOS(-1.D0)
      G = EE/EMASS              !gamma factor of electron
      B = 1.D0 - 0.5D0/G**2 - 0.125D0/G**2
      EPH_ERF = G*EPH*(1.D0-B*COS(THETA))
      if(eph_erf.le.0) print *,'transform_ic: eph_erf.le.0',eph_erf
      COSTHETA_ERF = (COS(THETA)-B)/(1.D0-B*COS(THETA))
      SINTHETA_ERF = SIN(THETA)/(G*(1.D0-B*COS(THETA)))
      SCAT_ANG = THETAM_IC(EPH_ERF) !sample the scattering angle
c      scat_ang = 1.d0
      EPRIME_ERF = EPH_ERF/(1.D0+EPH_ERF*(1.D0-COS(SCAT_ANG))/EMASS)
```

```
      R=RNUNF()
      R=RNUNF()
      PHI = R*2.D0*PI
      PXPRIME = COSTHETA_ERF*COS(SCAT_ANG)-SINTHETA_ERF*SIN(SCAT_ANG)
     &     *SIN(PHI)
      EPHNEW = G*EPRIME_ERF*(1.D0+B*PXPRIME)
      RETURN
      END

*******************************************************************

      FUNCTION THETAM_IC(EPH)
      IMPLICIT REAL*8(A-H,O-Z)
      DIMENSION ENERGY(500),THETAM(500)
      DATA IFIRST/1/

      IF (IFIRST.EQ.1) THEN
         ifirst = 0
         open (unit=12,file='thetam_ic.dat',status='old')
         read(12,*) nsize
         read(12,*) (energy(i),i=1,nsize)
         read(12,*) (thetam(i),i=1,nsize)
         close(unit=12)
      endif
      THETAM_IC=0.D0
c interpolate in array
      DELTA_EL = ENERGY(2)-ENERGY(1)
      EL = DLOG10(EPH)
      IE = (EL-ENERGY(1))/DELTA_EL + 1
      IF (IE.GT.NSIZE) IE=NSIZE-1
      IF (IE.LT.1) IE=1

      SLOPE = (THETAM(IE+1)-THETAM(IE))/DELTA_EL
      THETAM_IC = THETAM(IE) + SLOPE*(EL-ENERGY(IE))
      RETURN
      END
```

Appendix D

Mean free path and mean photon energy program

```
      PROGRAM GGEE_BB
C     MEAN FREE PATH (MPC) FOR PAIR PRODUCTION ON BLACK BODY
C     RADIATION OF TEMPERATURE T, AND MEAN SOFT PHOTON ENERGY (GEV)
C     ADAPTED FROM A PROGRAM BY R.J. PROTHEROE

      IMPLICIT REAL*8 (A-H,O-Z)
      PARAMETER (M=150)
      DIMENSION EMID(M),XINT(M),EBAR(M)
      DATA EMASS/0.5110034D-3/   ! ELECTRON MASS (GEV)
      DATA BK/8.617E-14/         ! BOLTZMANN CONST (GEV/K)
      DATA PC6/3.086D24/         ! 1 MPC IN CM

      T=2.728D0
      BKT=BK*T
      DO IP=1,M
         EMID(IP)=1.D0*10.D0**((IP-0.5D0)*0.1D0)
      ENDDO
      DO IP=1,M
         write(6,*)ip
         EM=EMID(IP)
         CALL PPMFP(EM,T,GGMFP,E)
         XINT(IP)=GGMFP/PC6
         ebar(ip)=e
      ENDDO
      k=0
 10   k=k+1
      if (ebar(k).eq.0.d0) goto 10
      k=k-1
      OPEN (UNIT=1, FILE='mbr_MFP.dat', STATUS= 'unknown')
      write(1,*) M
      WRITE(1,*) (DLOG10(EMID(I)), I=1,M)
      WRITE(1,*) (DLOG10(XINT(I)), I=1,M)
      close(unit=1)
      open (unit=2,file='mbr_ebarpp.dat',status='unknown')
```

```
      write(2,*) (m-k)
      write(2,*) (dlog10(emid(i)), i=k+1,m)
      WRITE(2,*) (dlog10(EBAR(I)),I=k+1,M)
      CLOSE (UNIT=2)

      STOP
      END
C==================================================================

      SUBROUTINE GGEE_SINT(SMAX,GGEE_SIGINT)
C
C     CALCULATES INTEGRAL OF S*SIGMA(S) OVER S FROM STHR TO SMAX
C     FOR PAIR PHOTOPRODUCTION.
C     SMAX IN GEV^2
C     UNIT: GEV^4 CM^2
C

      IMPLICIT REAL*8 (A-H,O-Q,S-Z)
      IMPLICIT REAL (R)
      DIMENSION SIGSINT(1000000)

      DATA IFIRST/1/
      DATA EMASS/0.5110034D-3/
      DATA DELTA/0.0001D0/

      STHR=(2*EMASS)**2
      IF(IFIRST.EQ.1)THEN
         IFIRST=0
         SUM=0.D0
         VAL=0.D0
         DLOGS=DELTA*2.3025851D0
         DO ISMAX=1,260000
            OLDVAL=VAL
            S=STHR*10.D0**(ISMAX*DELTA)
            VAL=S*(GGEETOT_CS(S))*S*DLOGS
            SUM=SUM+0.5D0*(OLDVAL+VAL)
            SIGSINT(ISMAX)=SUM
         ENDDO
      ENDIF

      GGEE_SIGINT=0.D0
      IF(SMAX.LE.STHR)RETURN
      SMAXL=DLOG10(SMAX/STHR)
      ISMAX=SMAXL/DELTA+1.D0
      IF(ISMAX.GT.260000) THEN
         WRITE(6,*)'GGEE_SIGINT(SMAX):
     &        (ISMAX.GT.150000).  ',SMAX,ISMAX
      ELSEIF(ISMAX.EQ.1)THEN
```

```
         GGEE_SIGINT=(SMAXL/DELTA+1.D0-ISMAX)*SIGSINT(ISMAX)
      ELSE
         GGEE_SIGINT=SIGSINT(ISMAX-1)+(SMAXL/DELTA+1.D0-ISMAX)*
     &        (SIGSINT(ISMAX)-SIGSINT(ISMAX-1))
      ENDIF
      GGEE_SIGINT=GGEE_SIGINT

      RETURN
      END

C ==================================================================

      SUBROUTINE PPMFP(EP,T,GGMFP,EBAR)
C
C     INTERACTION LENGTH (CM) OF PHOTONS IN BLACK BODY RADIATION
C     EP (GEV), T (K)

      IMPLICIT REAL*8 (A-H,O-Z)

      DATA BK/8.617E-14/,PI/3.14159D0/
      DATA EMASS/0.5110034d-3/

      BKT=BK*T
      DLOGEPH=0.01D0*2.3025851D0

      BETA=1.D0
      STHR=(2.d0*EMASS)**2
      EPHTHR=STHR/(2.D0*EP*(1.D0+BETA))

      SUM=0.D0
      AVSUM=0.D0
      DO IEPH=1,1000
         EPH=EPHTHR*10.D0**(0.01D0*IEPH)
         SMAX=2.D0*EPH*EP*(1.D0+BETA)
         CALL GGEE_SINT(SMAX,SINT,0,DUMMY)
         if (sint.le.0.d0) print *,'GGEE_SINT.LE.0.D0',sint,eph
         VAL = BB_DENS(EPH,BKT)*SINT*DLOGEPH/EPH
         SUM=SUM+VAL
         AVSUM=AVSUM+VAL*EPH
      ENDDO
      GGMFP=(8.D0*EP**2*BETA)*1.D80
      EBAR = AVSUM * 1.D80
      if (sum.lt.0.d0) print *,'GGEE_SINT:sum<0',sum,ep
      IF(SUM.GT.1.D-80) THEN
         GGMFP=(8.D0*EP**2*BETA)/SUM
         EBAR = AVSUM/SUM
      ENDIF
```

```
      RETURN
      END

C ==================================================================

      FUNCTION GGEETOT_CS(S)

      IMPLICIT REAL*8 (A-H,O-Z)

      DATA EMASS/0.5110034d-3/
      GGEETOT_CS=0.D0
      IF(S.LE.(2.D0*EMASS)**2)RETURN

      x = (2.D0*EMASS)**2/S     !1 - beta^2
      y = 0.5d0*x + 0.125*x**2  !1 - beta

      SIG=-2.D0*(1.d0-y)*(x+1.D0)+(2.d0+x*(2.d0-x))*DLOG((2.d0-y)/y)
      GGEETOT_CS=1.2474D-25*x*SIG

      return
      end

C ==============================================================

      DOUBLE PRECISION FUNCTION BB_DENS(E,KT)
C
C     GIVES DIFFERENTIAL NUMBER DENSITY OF PHOTONS IN A
C     BLACK BODY FIELD OF TEMPERATURE T (KELVIN)
C
C     UNITS PHOTONS CM^-3 GEV^-1
C
C     E: PHOTON ENERGY (GEV)
C     KT: (BOLTZMANN CONST)*T (GEV)
C

      IMPLICIT NONE
      DOUBLE PRECISION EKT,KT,E,FACTOR

      EKT=E/KT
      IF(EKT.LT.1.D-7)THEN
         FACTOR=1/(EKT+EKT**2/2+EKT**3/6)
      ELSE
         IF(EKT.LT.1.D2)THEN
            FACTOR=1.D0/(DEXP(EKT)-1.D0)
         ELSE
            FACTOR=0.D0
         ENDIF
      ENDIF
```

```
BB_DENS=1.31D40*E**2*FACTOR

RETURN
END
```

Appendix E

Median scattering angle program

```
      PROGRAM THETA_SAMPLE_PP2
C sample the mean scattering angle theta (called alpha in the
c thesis) in the centre of momentum frame for a
C photon-photon pair production interaction

      IMPLICIT REAL*8 (A-H,O-Z)
      PARAMETER(N=140)
      DIMENSION ENERGY(N),THETAM(N)
      DATA EMASS/0.51100337D-3/  ! ELECTRON MASS (GEV)

      DE = 0.05
      EMINLOG = DLOG10(EMASS)
      DO I=1,N
         print *,i
         ENERGY(I) = 10**(EMINLOG+DFLOAT(I)*DE)
         THETAM(I) = THETAM_PP(ENERGY(I))
      ENDDO

      OPEN(UNIT=9,FILE='thetam_pp.dat',STATUS='unknown')
      WRITE(9,*) N
      WRITE(9,*) (DLOG10(ENERGY(I)), I=1,N)
      WRITE(9,*) (THETAM(I), I=1,N)
      CLOSE(UNIT=9)
      END

*********************************************************************

      FUNCTION THETAM_PP(EPH)
      IMPLICIT REAL*8 (A-H,O-Z)
      PARAMETER(N=100000)
      DATA EMASS/0.51100337D-3/ ! ELECTRON MASS (GEV)
      DATA R/2.818d-13/         !classical radius of electron (cm)
      PI = DACOS(-1.D0)
      WM = EPH/EMASS
      IF (WM.LT.1) THEN
         THETAM_PP = 0.D0
```

```
         PRINT *,'THETAM_PP : EPH < EMASS'
         RETURN
      ELSE
         B = 1.D0 - 0.5D0/WM**2         !beta
         bsqd = 1.d0 - 1.d0/wm**2       !beta ^2
         IF (WM.LT.620) THEN
            SUM = 0.D0
            VAL = 0.D0
            DX = 1.D0/N
            X = 0.D0 - DX
            DO I=1,N+1
               X = X + DX
               VAL = 1.D0-Bsqd**2*X**4+2.D0*Bsqd/WM**2*(1-X**2)
               VAL = 0.5D0*PI*R**2 * B/(WM**2)*VAL/
     &              (1.D0-Bsqd**2*X**2)**2
               SUM = SUM + VAL*DX
            ENDDO
            if (sum.le.0.d0) print *,'THETAM_PP: SUM<0'
            HALFSUM = dlog10(sum/2.D0)
            THETAM_PP = 0.D0
            SUM = 0.D0
            VAL = 0.D0
            X = 0.D0 - DX
 30         CONTINUE
            if ((x+dx).gt.1.d0) then
               print *,'THETAM_PP:reached limit of x'
               goto 20
            endif
            X = X + DX
            VAL = 1.D0-Bsqd**2*X**4+2.D0*Bsqd/WM**2*(1-X**2)
            VAL = 0.5D0*PI*R**2 * B/(WM**2)*VAL/
     &           (1.D0-Bsqd**2*X**2)**2
            if (val.le.0.d0) print *,'THETAM_PP: VAL<0',val,x
            SUM = SUM + VAL*DX
            TOTALLOG = DLOG10(SUM)
            IF (TOTALLOG.GE.HALFSUM)THEN
               IF (ABS(TOTALLOG-HALFSUM).LT.0.0001) THEN
                  GOTO 20
               ELSE
                  SUM = SUM - VAL*DX
                  X=X-DX
                  DX = DX/10.D0
                  GOTO 30
               ENDIF
            ENDIF
            GOTO 30
 20         THETAM_PP = DACOS(X)
         ELSE
```

```
            TOLX = 1.D-6
            X = 0.5D0
            FOLD = DLOG(WM*(1.D0-Bsqd*X*X)) - B*(X-0.5D0)
            DX = 0.01D0
 40         CONTINUE
            X = X+DX
            FNEW = DLOG(WM*(1.D0-Bsqd*X*X)) - B*(X-0.5D0)
            IF ((FOLD*FNEW).LT.0.D0) THEN
               X=X-DX
               DX=DX/2.D0
            ENDIF
            IF (ABS(DX).GT.TOLX) GOTO 40
            THETAM_PP = DACOS(X)
         ENDIF
         RETURN
      ENDIF
      END
```